IEEE Access
Multidisciplinary | Rapid Review | Open Access Journal

Received November 16, 2019, accepted December 3, 2019, date of publication December 11, 2019,
date of current version December 23, 2019.

Digital Object Identifier 10.1109/ACCESS.2019.2958695

Centralized OPF in Unbalanced Multi-Phase Neutral Equipped Distribution Networks Hosting ZIP Loads

MUHAMMAD USMAN[1], (Member, IEEE), ANDREA CERVI[2], (Member, IEEE), MASSIMILANO COPPO[1], (Member, IEEE), FABIO BIGNUCOLO[1], (Member, IEEE), AND ROBERTO TURRI[1], (Senior Member, IEEE)

[1]Department of Industrial Engineering, University of Padova, 35131 Padua, Italy
[2]Interdepartmental Centre Giorgio Levi Cases for Energy Economics and Technology, University of Padova, 35131 Padua, Italy

Corresponding author: Muhammad Usman (muhammad.usman@studenti.unipd.it)

This work was supported by the University of Padova.

ABSTRACT The Optimal Power Flow (OPF) model for low voltage active Distribution Networks (DNs), which are equipped with neutral conductors, requires an explicit representation of both phases and neutral conductors in its formulation to obtain complete information about the state variables related to these conductors. In this regard, a centralized OPF relaxation based on semi-definite programming is presented in this paper for neutral-equipped DNs hosting ZIP loads and neutral-ground impedance, and contain a significant level of unbalance. The major restriction in the development of an OPF model for these networks is the coupled power injection across the conductors which is successfully handled by deriving the explicit active and reactive power injections for each conductor through a network admittance matrix-based approach. The shortcomings of existing voltage magnitude-based technique for the modelling of ZIP loads are comprehensively reported and a novel complex voltage variable-based approach is proposed which successfully incorporates ZIP loads in the developed multi-phase OPF relaxation. For the handling of constant current load, a modelling approach based on the first-order-Taylor series is introduced as well. Furthermore, the impact of the application of Kron reduction approach on the global optimal solution of single- and multiple-point grounded DNs is discussed in detail. Three metrics, eigenvalue ratio, power mismatch and cumulative normalized constraint violation, are utilized to evaluate the exactness of proposed relaxation. Simulations, carried out on several medium and low voltage DNs, show that the proposed relaxation is numerically exact under several combinations of ZIP load parameters and a reasonable range of grounding impedance value for both time-varying and extreme system loading scenarios irrespective of the degree of unbalance in a network.

INDEX TERMS Active distribution networks, optimal power flow, neutral conductor, semi-definite programming relaxation, ZIP loads.

ACRONYM

CCI	Correction Correction Injection
CNCV	Cumulative Normalized Constraint Violation
CT	Computational Time
DER	Distributed Energy Resource
DG	Distributed Generator
DN	Distribution Network
DNN	Distribution Network which is equipped with a Neutral conductor
EVR	Eigen Value Ratio
FR	Feasible Region
KR	Kron Reduction
LM	Load Model
LV	Low Voltage
MPG	Multiple Point Grounded
MPSDP	Multi-Phase Semi-Definite Programming
MV	Medium Voltage
OF	Objective Function

The associate editor coordinating the review of this manuscript and approving it for publication was Ziang Zhang.

OG	Optimality Gap
OP	Optimization Problem
OPF	Optimal Power Flow
OV	Optimization Variable
RD	Relative Difference
SDP	Semi-Definite Programming
SOCP	Second-Order-Cone-Programming
SPG	Single Point Grounded

I. INTRODUCTION

The rapid proliferation of renewable Distributed Energy Resources (DERs) in Distribution Networks (DNs), particularly Low Voltage (LV) networks, has raised several technical issues, such as voltage rise, voltage unbalance, reverse power flow etc., [1], which hinder the reliable and secure operation of these networks. Consequently, the optimal control and management of these networks have gained significant attention in the past decade to tackle these issues [2]–[4]. In this regard, AC-OPF, dynamic stability analysis and simulations, state estimation etc. are being considered as key tools for ensuring the efficient and safe operation of these networks. Among them, an immense effort has been put in solving the AC-OPF problem due to its non-linear, non-convex and NP-hard nature [5]. In this regard, a voluminous amount of literature is published on the solution algorithms, such as Newton-based methods [6], [7], linear and quadratic programming [8], non-linear and polynomial programming [9], interior point methods [10] and heuristic optimization techniques [11], for the single-phase equivalent AC-OPF problem. However, these deterministic and stochastic algorithms do not guarantee the global optimality and feasibility of the obtained solution due to the lack of sufficient criteria.

Recently, AC-OPF problem is reformulated as a convex Optimization Problem (OP) by leveraging tools from the convex optimization theory. These tools either relax or approximate the non-convex Feasible Region (FR) of the original problem into a convex FR and try to find the solution in the convexified region. In this context, Semi-Definite Programming (SDP) [12], [13], Second-Order-Cone-Programming (SOCP) [14], [15], quadratic convex [16], sequential convex [17], moment/sum-of-squares [18] -based single-phase equivalent OPF models have been developed. The global optimality of SDP-based relaxation for radial and mesh DNs has been proven in [19], [20] and [21], respectively, whereas the exactness of SDP- and SOCP-based OPF models are discussed in [22] and [23]. A detailed survey of these relaxations and approximations can be found in [24]. Due to large computational requirements of SDP-based relaxation, the sparsity of power networks is exploited in [25]–[28] which significantly reduces the Computational Time (CT) of this relaxation and, therefore, allows its practical realization for large-size networks.

To determine the optimal active and reactive power operational points of single- and three-phase DERs connected to Medium Voltage (MV) and/or LV DNs, it is incumbent to solve a multi-phase OPF model. Since these DNs exhibit significant unbalanced loading, solving a single-phase equivalent OPF model provides an incomplete picture of the state variables of these DNs. However, due to the increased complexity and non-convexity of a multi-phase OPF problem, in comparison to a single-phase equivalent OPF model, only few researchers have studied it for three-phase DNs. Among the convex relaxations, SDP- and SOCP-based approaches are extended in [29] and [30], [31], respectively for three-phase DNs, whereas, only quite recently, the chordal relaxation-based SDP models are developed in [32], [33] which exploit the sparsity of three-phase SDP-based relaxation to speed-up the computational process. It must be noted that due to complex analytical characterization of mutually coupled power injections in multi-phase unbalanced DNs, sufficient conditions related to the exactness of multi-phase OPF models do not exist yet.

The developed three-phase OPF models, however, depict some major shortcomings. Firstly, in all proposed models, only phase-ground decoupled power injections have been taken into consideration. However, in the case of a DN which is equipped with a Neutral conductor (DNN) and hosts shunt elements either between phase-neutral (wye) or phase-phase (delta) conductors, the assumption of phase-ground power injection is not applicable any more. In such network, the power injections are coupled between two conductors and, therefore, the decoupling of these injections is a must requirement in order to develop an OPF model for it. Secondly, in all the studies except [34], only constant power load has been taken into consideration. In [34], a full ZIP load model is taken into account in a single-phase equivalent SDP-based OPF model; however, it has been shown in this work that the approach reported in [34] cannot be generalized for the loads connected in a multi-phase DNN. Lastly, in [29], the Kron Reduction (KR) technique is utilized to implicitly add the impact of neutral conductor in the OPF model. However, in the case of Single Point Grounded (SPG) and Multiple Point Grounded (MPG) DNs, the unrealistic assumption of equipotential neutral conductor (which is the basis of KR approach) cannot be justified and, resultantly, it becomes necessary to model neutral conductors and neutral-ground impedance explicitly in a multi-phase OPF model.

A. CONTRIBUTIONS

In view of the above-mentioned shortcomings of the three-phase OPF models, the major contributions of this work can be categorized as:

- Proposal of a network admittance-based approach for the decoupling of coupled power injections between the conductors of a DNN and, subsequently, development of a centralized Multi-Phase SDP (MPSDP)-based OPF relaxation for such network
- Examining the limitations of existing voltage magnitude-based approach [34] and development of a novel complex voltage variable-based methodology for the

representation of a full ZIP load in the proposed OPF model
- Proposal of an approximate representation of the constant current component of a ZIP load in terms of the developed relaxation Optimization Variable (OV)
- Demonstrating the negative impact of the application of KR methodology on the quality of proposed relaxation in the case of SPG and MPG DNs

To achieve these objectives, a network admittance-based concept, Correction Current Injection (CCI) [35], [36], is employed which facilitates the representation of a shunt element by a constant admittance and a suitable current injector, and resultantly makes it possible to explicitly represent the power injections in each conductor of a DNN. For ZIP load(s), the current injection terms of CCI methodology are used to express the voltage dependency behaviour of constant impedance and constant current components. The constant impedance load dependency on the square of voltage magnitude term allows its easy handling in the OPF model; however, since constant current component depends on a absolute voltage magnitude term which is not available in the OV of existing three-phase SDP-based OPF relaxation, a modelling technique based on the *first-order Taylor series* is introduced to incorporate this load component in the proposed MPSDP-based OPF model.

Finally, it must be noted that for single-phase radial DNs, both SDP- and SOCP-based relaxations are equivalent and, therefore, one can solve the SOCP-based relaxation without making any compromise on the solution quality. However, as per authors knowledge, no such equivalence has been established between the primal SDP [29] and BIM-based SDP/BFM-based SDP [30], [31] relaxations in the case of three-phase DNs. Consequently, a general statement about the existence of equivalency between these relaxations would be an overstatement and, therefore, in this work SDP approach is utilized since it generalizes the SOCP technique.

B. STRUCTURE OF THE PAPER

The rest of the paper is organized as follows. Section II introduces the nomenclature and recalls the modelling of a three-phase SDP-based OPF relaxation. In section III, the decoupled power injections are developed and a brief note on the limitations of voltage-magnitude-based approach [34] is presented. Section IV presents a new complex voltage variable-based approach for incorporating ZIP loads, whereas, in section V, a complete MPSDP-based OPF model for DNNs is presented. Section VI reports the quality assessment of the proposed OPF relaxation and final remarks are concluded in section VII.

II. STANDARD THREE PHASE SDP-BASED AC-OPF MODEL

A. NOMENCLATURE

Consider a radial active DN comprising a set N of $n+1$ nodes as $N = \{0, 1, 2, \cdots, n\}$ and a set E of branches as $E = \{(i, j) \subset N \times N\}$ having τ conductors between any two nodes. Let 0 represents the slack node and define N^+ as $N\backslash\{0\}$. Consider $G \subseteq N$ be the set of DGs containing s units. Let $\phi_{ij} \subset \{a_{ij}, b_{ij}, c_{ij}, n_{1_{ij}}, \cdots, n_{w_{ij}}\}$ and $\phi_i \subset \{a_i, b_i, c_i, n_{1_i}, \cdots, n_{w_i}\}$ be the sets containing phase and neutral conductors of a line $(i, j) \in E$ and, phase and neutral conductors of a node $i \in N$, respectively. Consider $\delta_i \subset \{n_{1_i}, \cdots, n_{w_i}\}$ be the set containing neutral conductors of a node i and define $\eta_i = \phi_i\backslash\delta_i$ be the set containing only phase conductors. Consider $\psi_i \subset \{a_i{-}n_{1_i}, b_i{-}n_{1_i}, c_i{-}n_{1_i}, \cdots, a_i{-}n_{w_i}, b_i{-}n_{w_i}, c_i{-}n_{w_i}\}$ and $\chi_i \subset \{a_{ig}, b_{ig}, c_{ig}\}$ be the set of phase-neutral and phase-ground connection of a node i.

Consider $\mathbf{V}_i = [V_i^{ag}\ V_i^{bg}\ V_i^{cg}\ V_i^{n_1 g}\ \cdots\ V_i^{n_w g}]^T$ be the complex phase-ground voltage vector of a node i and define $\mathbf{V} = [\mathbf{V}_1, \cdots, \mathbf{V}_n]^T$ be the vector containing voltages of all nodes. For $\upsilon \in \psi_i$, let $P_{l_i}^{\upsilon}/P_{g_i}^{\upsilon}$ and $Q_{l_i}^{\upsilon}/Q_{g_i}^{\upsilon}$ represent the active and reactive power demand/generation of a load/DG connected between a particular phase and neutral of a node i having constant admittance $y_{l_i}^{\upsilon}/y_{g_i}^{\upsilon}$. For a DNN, define $y_{gnd_m}^{\alpha}$ be the admittance between neutral and ground of a node m for $\alpha \in \delta_m$, and finally, let $\underline{x}$ and $\overline{x}$ denote the lower and upper limits on a variable x, respectively.

B. CENTRALIZED THREE-PHASE SDP-BASED OPF RELAXATION

The standard SDP-based OPF model for three-phase DNs [29] is briefly recalled in model **M1** since it sets the basis of this work. For detailed understanding of this approach, please refer to [29].

M1: Three-Phase SDP-Based OPF Model

variable : $\mathbf{W} = \mathbf{V}\mathbf{V}^{\mathbf{H}}$

subject to :

$$\mathrm{Tr}(\Psi_{k,nw_{p/q}}^{\varphi}\mathbf{W}) + P_{l_k}^{\upsilon}/Q_{l_k}^{\upsilon} = 0, \quad \forall\varphi \in \eta_k, \upsilon \in \chi_k, k \in N\backslash G \tag{1a}$$

$$\underline{P}_{g_i}/\underline{Q}_{g_i} \leq \mathrm{Tr}(\Psi_{i,nw_{p/q}}^{\varphi}\mathbf{W}) + P_{l_i}^{\upsilon}/Q_{l_i}^{\upsilon} \leq \overline{P}_{g_i}/\overline{Q}_{g_i}, \quad \forall\varphi \in \eta_i, \upsilon \in \chi_i, i \in G \tag{1b}$$

$$|\underline{V}_k|^2 \leq \mathrm{Tr}(\Psi_{k,nw_v}^{\varphi}\mathbf{W}) \leq |\overline{V}_k|^2 \quad \forall\varphi \in \eta_k, k \in N^+ \tag{1c}$$

$$\mathbf{W} \succeq 0 \tag{1d}$$

$$\mathrm{rank}(\mathbf{W}) = 1 \tag{1e}$$

It can be noticed that constraints (1a)-(1c) are linear with respect to $\mathbf{W}$ and are, therefore, convex. The non-convexity of model **M1** is restricted to (1e) which can be dropped to make it a convex OPF model. Please note that the voltage vector $\mathbf{V}$ in **M1** contains only phases voltages. Two key observations can be noticed in the model **M1**:

1) In (1a)-(1b), phase-ground power injections $(P_{l/g}, Q_{l/g})$ are considered. Consequently, the injection at each phase of a node becomes decoupled from the injection at other phases of the same node.

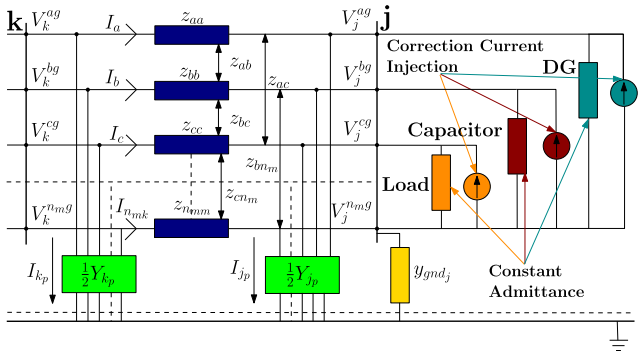

FIGURE 1. Distribution network representation with constant load admittances, correction current injections and earthing admittance.

2) Constant power loads are considered in (1a)-(1b). In fact, as stated earlier in section I, the published literature on the convex relaxation-based OPF models, except [34], has considered this load type due to the fact that its power absorption is voltage independent and, therefore, can be easily incorporated in an OPF model. In [34], ZIP loads are handled in the framework of an equivalent single-phase representation of an electrical network; however, it is comprehensively demonstrated in section III-B that such modelling technique fails to correctly take into account the behaviour of a ZIP load in the case of multi-phase SPG and MPG DNs.

In the case of neutral-equipped DNs, shunt elements are connected either between phase-phase or phase-neutral conductors and, consequently, model **M1** cannot simply be extended to these networks by specifying additional power balance equalities related to the neutral conductor(s) due to the existence of coupled power injections. Furthermore, the OPF model for such networks must be able to correctly capture the behaviour of a complete ZIP load. This is due to the fact that constant impedance and constant current loads are part of the overall connected load and ignoring the impact of their voltage dependency can lead to sub-optimal results. These shortcomings are thoroughly tackled in the next sections where explicit power injections are developed for each conductor of a network through CCI approach. Furthermore, a novel complex voltage variable-based methodology is also introduced to incorporate a ZIP load in the proposed MPSDP-based OPF relaxation.

III. SDP-BASED OPF METHODOLOGY FOR MULTI-PHASE NETWORKS CONTAINING NEUTRAL CONDUCTORS

Consider a typical branch of a 4-wire DN incorporating loads, DGs and grounding impedance as shown in Fig. 1. Please note that for the sake of clarity, only one neutral conductor is considered in the subsequent derivation. Nevertheless, the presented approach can easily be generalized for any number of neutral conductors. The key concept in the CCI approach is the representation of any shunt element by a combination of a constant admittance and a suitable current injector, if required. The advantage of this methodology is that constant admittance part can be easily incorporated in the bus admittance matrix whereas the voltage dependency of a shunt element can be customized in terms of a current injection term based upon its chosen model i.e., *Z*, *I* or *P*. On the basis of this approach, the apparent power of a single-phase shunt element can be written as:

$$S^{*\upsilon}_{i_{(r)}} = Y^{\upsilon}_{i_{(0)}} |V^{\upsilon}_{i_{(r)}}|^2 - V^{\upsilon}_{i_{(r)}} \Delta I^{\upsilon}_{i_{(r)}} \tag{2}$$

where $i \in N$, $\upsilon \in \psi_i$, ΔI is current injection and $Y^{\upsilon}_{i_0}$ is defined as:

$$Y^{\upsilon}_{i_{(0)}} = \frac{S^{*\upsilon}_{i_{(0)}}}{|V^{\upsilon}_{i_{(0)}}|^2}, \tag{3}$$

where subscript (0) refers to the rated value. It can be noticed that shunt-element admittance is based on the rated apparent power and voltage values and is, therefore, constant, whereas the voltage dependency of each of its component can be defined as follows:

$$\text{Z: } \Delta I^{\upsilon:Z\%}_{i_{(r)}} = 0 \tag{4}$$

$$\text{I: } \Delta I^{\upsilon:I\%}_{i_{(r)}} = k_I \frac{Y^{\upsilon}_{i_{(0)}}}{V^{\upsilon}_{i_{(r)}}} (|V^{\upsilon}_{i_{(r)}}|^2 - |V^{\upsilon}_{i_{(r)}}||V^{\upsilon}_{i_{(0)}}|) \tag{5}$$

$$\text{P: } \Delta I^{\upsilon:P\%}_{i_{(r)}} = k_P \frac{Y^{\upsilon}_{i_{(0)}}}{V^{\upsilon}_{i_{(r)}}} (|V^{\upsilon}_{i_{(r)}}|^2 - |V^{\upsilon}_{i_{(0)}}|^2) \tag{6}$$

By substituting (4)-(6) in (2), the apparent power corresponding to each component of a single-phase shunt element becomes:

$$S^{*\upsilon:Z\%}_{i_{(r)}} = k_Z \cdot Y^{\upsilon:Z\%}_{i_{(0)}} |V^{\upsilon}_{i_{(r)}}|^2 \tag{7a}$$

$$S^{*\upsilon:I\%}_{i_{(r)}} = (1-k_I) \cdot Y^{\upsilon:I\%}_{i_{(0)}} |V^{\upsilon}_{i_{(r)}}|^2 + k_I Y^{\upsilon}_{i_{(0)}} (|V^{\upsilon}_{i_{(r)}}||V^{\upsilon}_{i_{(0)}}|) \tag{7b}$$

$$S^{*\upsilon:P\%}_{i_{(r)}} = (1-k_P) \cdot Y^{\upsilon:P\%}_{i_{(0)}} |V^{\upsilon}_{i_{(r)}}|^2 + k_p Y^{\upsilon}_{i_{(0)}} |V^{\upsilon}_{i_{(0)}}|^2 \tag{7c}$$

where $Y^{\upsilon:(Z/I/P)\%}_{i_{(0)}}$ represent the constant admittance terms related to each component of a ZIP load at node *i*. The parameters k_Z, k_I and k_P represent the coefficients corresponding to active/reactive power injection of constant impedance, constant current and constant power components. The subscript *r* represents the rth-iteration of a CCI-based load flow. However, in the case of OPF model, it becomes irrelevant and, therefore, has been dropped in the subsequent formulations. It must be noted that in (7a)-(7c), the same voltage dependency for active and reactive power is considered to derive a compact form of the power injections, and subsequently, the OPF model. However, during real-time application of the proposed scheme, the active and reactive power injections related to each component of a ZIP load are multiplied by the respective active $k_{(Z/I/P)_p}$ and reactive $k_{(Z/I/P)_q}$ power parameters so that their correct voltage dependency can be taken into account.

A. DECOUPLING OF POWER INJECTION BETWEEN PHASES AND NEUTRAL CONDUCTORS

The apparent powers expressed in (7a)-(7c) do not represent the explicit power injections in phases and neutral conductors due to the presence of coupled admittance between them. This indicates that the whole problem of an OPF model development is reduced to split the admittance between the phases and neutral conductors which can be achieved by defining a load matrix Λ_i for each node i of the network as follows:

$$\Lambda_i = \tilde{I}^T * \text{diag}(\hat{L}_i) * \tilde{I} \tag{8}$$

where $\tilde{I}$ is an incidence matrix and is defined as:

$$\tilde{I} = \begin{bmatrix} 1 & 0 & 0 & -1 \\ 0 & 1 & 0 & -1 \\ 0 & 0 & 1 & -1 \end{bmatrix}$$

and $\hat{L}_i = [Y^{an}_{i_{(0)}} Y^{bn}_{i_{(0)}} Y^{cn}_{i_{(0)}}]^T$ is a 3×1 vector containing rated admittances of shunt elements connected between phases and neutral conductors of a node i. Through Λ_i, the explicit power injections corresponding to each component of a ZIP load at node i become:

$$\mathbf{S}^{*Z\%}_i = \mathbf{V}^*_i \otimes \{\Lambda^Z_i \mathbf{V}_i\} \tag{9}$$

$$\mathbf{S}^{*I\%}_i = \mathbf{V}^*_i \otimes \{(\Lambda^{I_c}_i - \Lambda^I_i)\mathbf{V}_i\} + \Lambda^I_i(|\mathbf{V}_i| \otimes |\mathbf{V}_{i_{(0)}}|) \tag{10}$$

$$\mathbf{S}^{*P\%}_i = \mathbf{V}^*_i \otimes \{(\Lambda^{P_c}_i - \Lambda^P_i)V_i\} + \mathbf{V}^*_{i_{(0)}} \otimes \{\Lambda^P_i \mathbf{V}_{i_{(0)}}\} \tag{11}$$

where $\Lambda^{I_c}_i$, $\Lambda^{P_c}_i$ are load matrices which are independent of ZIP parameters, whereas load matrices Λ^Z_i, Λ^I_i, Λ^P_i are formed by multiplying k_Z, k_I and k_P to the respective load components. $\mathbf{S}^*_i$ is a 4×1 vector representing apparent power injection at each conductor of a node i and subscript (0) indicates the initial voltage value at each node. It can now be observed that for a single-phase load connected between phase a and neutral n, the decoupled power injection in these conductors, for a constant impedance component, can be expressed as:

$$S^{*ag}_i = Y^{an}_i * |V_{ag_i}|^2 - Y^{an}_i * \{V^*_{ag_i} V_{ng_i}\} \tag{12a}$$

$$S^{*ng}_i = -Y^{an}_i * \{V^*_{ng_i} V_{ag_i}\} + Y^{an}_i * |V_{ng_i}|^2 \tag{12b}$$

where voltages are referred to ground g. Eqs. (9)-(11) show how decoupled power injections for each component of a ZIP load can be obtained. After obtaining these injections, the last step towards establishing a multi-phase OPF model is to express them in terms of an OV and, subsequently, add them in the proposed relaxation. However, as shown in the next section, the approach reported in [34] is unable to handle ZIP loads in a multi-phase modelling environment due to the lack of availability of complex voltage variables. Consequently, we have proposed a new methodology which generalizes the ZIP load representation in both single- and multi-phase representation of an electrical network.

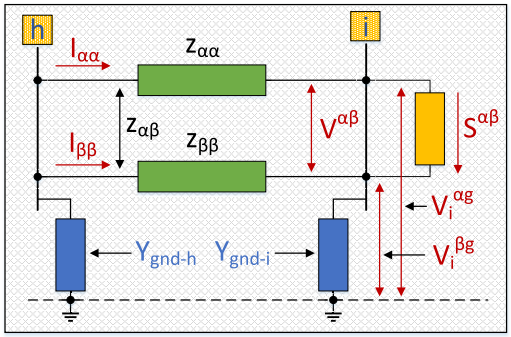

FIGURE 2. A fictitious MPG-DN containing a load between two floating potential phases.

B. LIMITATIONS OF VOLTAGE MAGNITUDE-BASED APPROACH FOR THE REPRESENTATION OF A ZIP LOAD

To incorporate the ZIP load, [34] has introduced an additional 2×2 rank-1 matrix Π_i (13) at each load bus i.

$$\Pi_i = \begin{bmatrix} 1 & |V_i| \\ |V_i| & |V_i|^2 \end{bmatrix} \tag{13}$$

The matrix Π_i, which contains the voltage magnitude terms $|V_i|$, allows to model the constant impedance and constant power components accurately. However, constant current element can only be represented approximately through it. Please refer to [34] for detailed understanding of this approach. For single-phase equivalent representation of electrical networks, the apparent power injection of a ZIP load can be represented as:

$$S(V_i) = k_Z * |V_i|^2 + k_I * |V_i| + k_P \tag{14}$$

which can be successfully handled by Π_i. For such networks, voltage V_i is referred with respect to the ground which is at a fixed potential. However, in the case of a multi-phase DN hosting shunt elements between two floating potential conductors, even the modelling of constant impedance part, which is considered pretty straight forward in the case of single-phase equivalently represented electrical networks, cannot be done through (13) as explained below.

Consider a simple two-phase DN, as shown in Fig. (2), which is grounded through a finite impedance and contains a shunt element between phases α and β. For the sake of clarity, only constant impedance load is considered. For such load type, the apparent power flowing through it can be expressed as:

$$S^{*\alpha\beta}_i(V_i) = k_Z * \frac{S^{*\alpha\beta}_{i_{(0)}}}{|V^{\alpha\beta}_{i_{(0)}}|^2} * |V^{\alpha\beta}_i|^2 \tag{15}$$

which, apart from being coupled between phases α and β, depends on a voltage term which is absent in the OV $\mathbf{W}$. However, by expressing $|V^{\alpha\beta}_i|^2$ as the product of two complex numbers;

$$|V^{\alpha\beta}_i|^2 = |V^{\alpha g}_i - V^{\beta g}_i|^2 = (V^{\alpha g}_i - V^{\beta g}_i) * (V^{\alpha g}_i - V^{\beta g}_i)^* \tag{16}$$

(15) can be expressed in terms of active and reactive power separately as shown in (17)-(18) for phase α.

$$P_i^{\alpha g} = Y_{i_R}^{\alpha\beta}(V_i^{\alpha g} * V_i^{\alpha g*}) + \left\{\frac{-Y_{i_R}^{\alpha\beta} + jY_{i_{Im}}^{\alpha\beta}}{2}\right\}(V_i^{\alpha g*} * V_i^{\beta g}) + \left\{\frac{-Y_{i_R}^{\alpha\beta} - jY_{i_{Im}}^{\alpha\beta}}{2}\right\}(V_i^{\alpha g} * V_i^{\beta g*}) \quad (17)$$

$$Q_i^{\alpha g} = -Y_{i_{Im}}^{\alpha\beta}(V_i^{\alpha g} * V_i^{\alpha g*}) + \left\{\frac{Y_{i_{Im}}^{\alpha\beta} + jY_{i_R}^{\alpha\beta}}{2}\right\}(V_i^{\alpha g*} * V_i^{\beta g}) + \left\{\frac{Y_{i_{Im}}^{\alpha\beta} - jY_{i_R}^{\alpha\beta}}{2}\right\}(V_i^{\alpha g} * V_i^{\beta g*}) \quad (18)$$

where R and Im represent the real and imaginary parts of a complex quantity. It can be clearly seen in (17)-(18) that besides the square of voltage magnitude term ($|V_i^{\alpha g}|^2$), $P_i^{\alpha g}/Q_i^{\alpha g}$ also depends on the product of two complex voltages. Since $(V_i^{\alpha g*} * V_i^{\beta g}) \neq (V_i^{\alpha g} * V_i^{\beta g*}) \neq |V_i^{\alpha g}||V_i^{\beta g}|$, (17)-(18) cannot be represented by (13) due to the absence of complex voltage variables in Π_i and, consequently, the approach presented in [34] cannot be generalized for ZIP loads connected in a multi-phase DN exhibiting high levels of unbalance i.e., significant neutral voltage with respect to the earth potential.

IV. COMPLEX VOLTAGE VARIABLE-BASED MODELLING FOR THE REPRESENTATION OF ZIP LOAD

To incorporate the decoupled power injections (9-11) in MPSDP-based OP relaxation, the following new OV $\hat{\mathbf{W}}$ is adopted in this work.

$$\hat{\mathbf{W}} = \begin{bmatrix}1\\ \mathbf{V}\end{bmatrix}\begin{bmatrix}1 & \mathbf{V}^H\end{bmatrix} = \begin{bmatrix}1 & \mathbf{V}^H\\ \mathbf{V} & \mathbf{W}\end{bmatrix} \quad (19)$$

As can be seen, $\hat{\mathbf{W}}$ contains both linear (first row and first column) and product of the complex voltage ($\mathbf{W}$ block) terms. Resultantly, each component of a ZIP load can be expressed through $\hat{\mathbf{W}}$. With the introduction of this new OV, there is no need to specify additional rank-1 matrices at each load bus and, consequently, set the positive semi-definiteness condition and coupling constraints on these matrices as done in [34] which ultimately simplifies the multi-phase OPF model. It is worth mentioning that the proposed approach generalizes the voltage magnitude scheme and can be successfully applied even in the case of single-phase equivalent representation of DNs.

A. REPRESENTATION OF CONSTANT IMPEDANCE AND CONSTANT POWER ELEMENTS

The representation of constant impedance (9) and constant power (11) injections is pretty straight-forward due to the presence of the square of voltage magnitude terms in their formulation which, in turn, are readily available in the $\mathbf{W}$ part of the OV $\hat{\mathbf{W}}$. To express the power injections, the following matrices are introduced.

$$\Gamma_{k,l}^{\varphi:P\%} = \mathbf{e}_k^{\varphi} * \mathbf{e}_k^{\varphi T} * \mathbf{Y}_L^P \quad \forall\varphi \in \phi_k,\ \forall k \in N \quad (20a)$$

$$\Psi_{k,l_p}^{\varphi:P\%} = \frac{1}{2}\{\Gamma_{k,l}^{\varphi:P\%} + (\Gamma_{k,l}^{\varphi:P\%})^H\} \quad \forall\varphi \in \phi_k,\ \forall k \in N \quad (20b)$$

$$\Psi_{k,l_q}^{\varphi:P\%} = \frac{j}{2}\{\Gamma_{k,l}^{\varphi:P\%} - (\Gamma_{k,l}^{\varphi:P\%})^H\} \quad \forall\varphi \in \phi_k,\ \forall k \in N \quad (20c)$$

where $\mathbf{Y}_L^P$ is the load matrix formed by Λ_i^P of all nodes, $\Psi_{k,l_p}^{\varphi:P\%}/\Psi_{k,l_q}^{\varphi:P\%}$ are the Hermitian matrices related to the active/reactive power injections and $\mathbf{e}_k^{\varphi}$ denotes the standard canonical basis of $\mathbb{R}^{|\phi_k|\times 1}$ and is defined as $\mathbf{e}_k^{\varphi} = [\mathbf{0}_{|\phi_0|}^T, \cdots, \mathbf{0}_{|\phi_{k-1}|}^T, \mathbf{I}_{|\phi_k|}^{\varphi T}, \mathbf{0}_{|\phi_{k+1}|}^T, \cdots, \mathbf{0}_{|\phi_n|}^T]^T$. Based upon these matrices, the active and reactive power injections in (11) become:

$$P_{k,l}^{\varphi:P\%} = \mathrm{Tr}(\Psi_{k,l_p}^{\varphi:P_c\%}\mathbf{W}) - \mathrm{Tr}(\Psi_{k,l_p}^{\varphi:P\%}\mathbf{W}) + \mathrm{Tr}(\Psi_{k,l_p}^{\varphi:P\%}\mathbf{W}_0) \quad (21a)$$

$$Q_{k,l}^{\varphi:P\%} = \mathrm{Tr}(\Psi_{k,l_q}^{\varphi:P_c\%}\mathbf{W}) - \mathrm{Tr}(\Psi_{k,l_q}^{\varphi:P\%}\mathbf{W}) + \mathrm{Tr}(\Psi_{k,l_q}^{\varphi:P\%}\mathbf{W}_0) \quad (21b)$$

where $\mathbf{W}_0 = \mathbf{V}_0\mathbf{V}_0^H$ and $\mathbf{V}_0$ is defined as the vector of initial voltages at all nodes.

On a similar basis, the injections related to constant impedance part, as shown in (22a)-(22b), can be defined by replacing $\mathbf{Y}_L^P$ with $\mathbf{Y}_L^Z$ (formed by Λ_i^Z) in (20a) and omitting $\mathrm{Tr}(\Psi_{k,l_{p/q}}^{\varphi:P_c\%}\mathbf{W})$and $\mathrm{Tr}(\Psi_{k,l_{p/q}}^{\varphi:P\%}\mathbf{W}_0)$ parts from (21a) and (21b), respectively.

$$P_{k,l}^{\varphi:Z\%} = \mathrm{Tr}(\Psi_{k,l_p}^{\varphi:Z\%}\mathbf{W}) \quad (22a)$$

$$Q_{k,l}^{\varphi:Z\%} = \mathrm{Tr}(\Psi_{k,l_q}^{\varphi:Z\%}\mathbf{W}) \quad (22b)$$

B. REPRESENTATION OF CONSTANT CURRENT ELEMENT

The injection related to constant current component contains both absolute and square of the voltage magnitude terms in its formulation as shown below.

- Square of the voltage magnitude term $\Rightarrow \mathbf{V}_i^* \otimes \{(\Lambda_i^{I_c} - \Lambda_i^I)\mathbf{V}_i\}$
- Absolute voltage magnitude term $\Rightarrow \mathbf{V}_i^* \otimes \Lambda_i^I(|\mathbf{V}_i| \otimes |\mathbf{V}_{i_{(0)}}|)$

The first part i.e., the square of voltage magnitude term, is similar to the constant power and constant impedance parts and can, therefore, be expressed in a similar fashion by replacing $\mathbf{Y}_L^P$ with $\mathbf{Y}_L^I$ (formed by Λ_i^I) in (20a). The second part, however, contains a voltage magnitude term which is not available in $\hat{\mathbf{W}}$. Consequently, a modelling formulation based on the *first-order Taylor series* is proposed to express the complete injection related to the constant current component in terms of $\hat{\mathbf{W}}$.

To express this part, consider the last term in (7b) for a load connected between phase a and neutral n of node i.

$$S_i^{*an} = k_I Y_{i(0)}^{an}\{|V_i^{an}| \cdot |V_{i(0)}^{an}|\} = k_I Y_{i(0)}^{an}\left\{\sqrt{(V_{i_R}^{ag} - V_{i_R}^{ng})^2 + (V_{i_{IM}}^{ag} - V_{i_{IM}}^{ng})^2}\right\} \quad (23)$$

$$S_i^{*an} \approx k_I Y_{i(0)}^{an}\{V_{i_R}^{ag} - V_{i_R}^{ng}\} + k_I Y_{i(0)}^{an}\{V_{i_{IM}}^{ag} - V_{i_{IM}}^{ng}\} \quad (24)$$

$$S_i^{*an} = k_I Y_{i(0)}^{an}\{V_{i_R}^{ag} + V_{i_{IM}}^{ag}\} - k_I Y_{i(0)}^{an}\{V_{i_R}^{ng} + V_{i_{IM}}^{ng}\} \quad (25)$$

It can be noticed that (24) is obtained through the first-order Taylor series which is evaluated at V_{a_0}. Based on (25),

the power injected into phase a and neutral n can be expressed as:

$$S_i^{*ag} = k_I Y_{i_{(0)}}^{an}\left(\frac{V_i^{ag}+V_i^{ag*}}{2}\right) + j * k_I Y_{i_{(0)}}^{an}\left(\frac{-V_i^{ag}+V_i^{ag*}}{2}\right) \quad (26)$$

$$S_i^{*ng} = k_I Y_{i_{(0)}}^{an}\left(\frac{V_i^{ng}+V_i^{ng*}}{2}\right) + j * k_I Y_{i_{(0)}}^{an}\left(\frac{-V_i^{ng}+V_i^{ng*}}{2}\right) \quad (27)$$

It can be noted that (26)-(27) involve the subtraction of voltage terms which can lead to poor numerical input data to the optimization solver due to the fact that computing softwares, such as MATLAB, do not produce a hard zero and, consequently, an extremely small number ($< 10^{-7}$) causes the solver either to report numerical problem in the optimization model or to produce sub-optimal results or to make the OP infeasible. Fortunately, the second term in (26) and (27) belongs to the imaginary component of a phase and neutral voltage, and can be dropped under the assumption that in the case of lightly and moderately unbalanced DNs, this term would be small as compared to the real component of these voltages. Moreover, the term $(V_{i_{Im}}^{ag} - V_{i_{Im}}^{ng})$ in (24) can also be ignored in the case of wye-connected loads in these DNs since the imaginary component of a neutral voltage becomes extremely small in comparison to the imaginary component of a phase voltage under such scenario i.e., $V_{i_{Im}}^{ng} \ll V_{i_{Im}}^{ag}$. Under these assumptions, the explicit power injections at phase a and neutral n can be expressed as:

$$S_i^{*ag} = k_I Y_{i_{(0)}}^{an}\left(\frac{V_i^{ag}+V_i^{ag*}}{2}\right) \quad (28)$$

$$S_i^{*ng} = -k_I Y_{i_{(0)}}^{an}\left(\frac{V_i^{ng}+V_i^{ng*}}{2}\right) \quad (29)$$

However, it must be emphasized that for highly unbalanced DNs, this assumption would lead to sub-optimal results. Before proceeding further, it is important to mention that in order to develop (28) for other phases b and c, their voltage vectors in $\hat{\mathbf{W}}$ must be rotated towards the reference position of phase a to have the same equivalent power injection in these phases corresponding to the same load attached to them as connected to the phase a.

The injections in (28)-(29) can readily be seen as the decoupled injections which can be expressed through $\hat{\mathbf{W}}$ by introducing the following matrix.

$$\Upsilon_{k,l}^{\varphi:I\%} = \hat{\Theta}_k * \mathbf{e}_k^{\varphi} * \mathbf{e}_k^{\varphi T} * \mathbf{Y}_L^{I_D} \quad \forall \varphi \in \phi_k,\ \forall k \in N \quad (30)$$

where $\hat{\Theta}_k$ is defined as:

$$\hat{\Theta}_k = \begin{bmatrix} \mathbf{0}_{11} & \cdots & \mathbf{c}_{1k}^{a} * \mathbf{c}_{1k}^{\varphi T} & \cdots & \mathbf{0}_{1n} \\ \vdots & \ddots & \vdots & \ddots & \vdots \\ \mathbf{0}_{n1} & \cdots & \mathbf{0}_{nk} & \cdots & \mathbf{0}_{nn} \end{bmatrix} \quad (31)$$

and $\mathbf{c}_k^{\varphi}$ is a standard canonical basis vector of $\mathbb{R}^{|\phi_k|\times 1}$ corresponding to phase φ. Based on (19) and (30), the active and reactive power injections corresponding to (28) for phase a can be written as:

$$P_k^{a:I_{Abs}} = \mathrm{Tr}\left\{\frac{\Re(\Upsilon_{k,l}^{a:I\%} + \Upsilon_{k,l}^{a:I\%^T})}{2}\hat{\mathbf{W}}\right\} \quad (32a)$$

$$Q_k^{a:I_{Abs}} = \mathrm{Tr}\left\{\frac{-\Im(\Upsilon_{k,l}^{a:I\%} + \Upsilon_{k,l}^{a:I\%^T})}{2}\hat{\mathbf{W}}\right\} \quad (32b)$$

In a similar fashion, the expressions for active and reactive power injections can be derived for other phases and neutral conductors as well. The complete injections related to constant current element can now be expressed as:

$$P_{k,l}^{\varphi:I\%} = \mathrm{Tr}(\Psi_{k,l_p}^{\varphi:I_c\%}\mathbf{W}) - \mathrm{Tr}(\Psi_{k,l_p}^{\varphi:I\%}\mathbf{W}) + P_{k_{(r)}}^{\varphi:I_{Abs}} \quad (33a)$$

$$Q_{k,l}^{\varphi:I\%} = \mathrm{Tr}(\Psi_{k,l_q}^{\varphi:I_c\%}\mathbf{W}) - \mathrm{Tr}(\Psi_{k,l_q}^{\varphi:I\%}\mathbf{W}) + Q_{k_{(r)}}^{\varphi:I_{Abs}} \quad (33b)$$

It has to be noted that the diagonal entry in (30) for a neutral conductor must be removed before developing injections (32a)-(32b) since it does not appear in the neutral component of (29).

C. INCORPORATION OF GROUNDING IMPEDANCE

In [37], it has been assumed that the neutral conductor is solidly grounded at each node in a multi-phase DN and, therefore, its impact can be implicitly taken into account through the application of KR methodology. However, this leads to the non-availability of neutral conductor state variables such as voltages and current. Furthermore, in the case of SPG and MPG DNs, the application of KR approach cannot be justified due to the existence of significant neutral voltages and current in this conductor [38], [39]. Therefore, in this work, the grounding impedance connected between a neutral conductor and ground is considered explicitly and, resultantly, the power injections related to it, as expressed below, are incorporated in the proposed OPF model.

$$P_{k,gnd}^{\varphi} = \mathrm{Tr}(\Psi_{k,gnd_p}^{\varphi}\mathbf{W}) \quad (34a)$$

$$Q_{k,gnd}^{\varphi} = \mathrm{Tr}(\Psi_{k,gnd_q}^{\varphi}\mathbf{W}) \quad (34b)$$

where $\Psi_{k,gnd_p}^{\varphi}/\Psi_{k,gnd_q}^{\varphi}$ are determined from (20b)-(20c) by replacing $\mathbf{Y}_L^P$ with $\mathbf{Y}_{gnd}$ in (20a) where $\mathbf{Y}_{gnd}$ is the neutral-ground admittance matrix.

V. MULTI-PHASE SDP-BASED OPF MODEL

The centralized MPSDP-based OPF model for DNNs can now be expressed since all active and reactive power injections corresponding to a full ZIP load have been represented explicitly for each phase and neutral conductor. However, it must be noted that all power injections except those shown in (32a)-(32b) must be expressed using $\hat{\mathbf{W}}$ instead of $\mathbf{W}$ which can be easily done by appending all Hermitian matrices of the corresponding active and reactive power injections with an additional row and column of zeros. Based on $\hat{\mathbf{W}}$ and extended Hermitian matrices, the resultant injections for a

TABLE 1. Quality of the proposed MPSDP-based OPF relaxation for $R_{gnd} = 1\Omega$.

LM	Load Parameters						Eigenvalue Ratio $\lvert\lambda_{P-1}\rvert/\lvert\lambda_P\rvert \times 10^{-5}$					Computational Time (s)				
	P_L			Q_L			MG	IT-37	IT-111†	CIGRE	IEEE	MG	IT-37	IT-111†	CIGRE	IEEE
	k_Z	k_I	k_P	k_Z	k_I	k_P	*LuB*	*MuB*	*MuB*	*HuB*	*HuB*	*LuB*	*MuB*	*MuB*	*HuB*	*HuB*
OF:1 Slack Bus Power (kVA)																
LM:1	1	0	0	1	0	0	0.17	0.34	6.43	1.09	0.66	2.1	1257	1.4	3.6	4.8
LM:2	0	1	0	0	1	0	0.12	1.34	3.18	1.02	0.54	2.5	1023	1.4	3.9	5.2
LM:3	0	0	1	0	0	1	0.07	0.84	2.33	0.72	1.50	1.8	1397	1.5	4.3	4.5
LM:4	1.56	-2.49	1.93	10.1	-16.75	7.65	0.10	1.96	6.93	**13.1**	3.26	2.1	1571	1.7	4.0	5.8
LM:5	0.57	-0.22	0.65	0.57	-0.22	0.65	0.03	0.56	0.89	0.77	1.36	1.6	1608	1.4	4.3	5.0
LM:6	1.21	-1.61	1.41	4.35	-7.08	3.72	0.10	1.47	1.32	7.03	**11.4**	1.7	1835	1.5	3.8	5.7
LM:7	1.21	-1.61	1.41	1.21	-1.61	1.41	0.10	0.44	1.87	3.11	1.34	2.1	1307	1.5	4.1	5.9
OF:2 Network Losses (kW)																
LM:1	1	0	0	1	0	0	0.04	1.50	6.66	6.95	3.71	1.6	1411	1.5	3.9	4.9
LM:2	0	1	0	0	1	0	0.34	0.48	5.09	1.90	0.75	1.4	1458	1.5	4.6	5.5
LM:3	0	0	1	0	0	1	0.23	0.43	6.96	0.42	0.36	1.5	1760	1.6	4.0	5.1
LM:4	1.56	-2.49	1.93	10.1	-16.75	7.65	0.16	0.43	9.20	1.46	**30.0**	1.5	1247	1.8	3.7	6.4
LM:5	0.57	-0.22	0.65	0.57	-0.22	0.65	0.17	0.22	8.91	2.31	2.51	1.8	1407	1.5	3.6	5.1
LM:6	1.21	-1.61	1.41	4.35	-7.08	3.72	0.28	0.90	9.07	2.37	**32.0**	1.7	1514	1.6	3.7	5.9
LM:7	1.21	-1.61	1.41	1.21	-1.61	1.41	0.02	0.25	6.60	1.13	1.01	1.7	1535	1.7	3.6	6.0

LM: Load Model MG: Micro Grid IT: Italian †: Memory Limit *LuB*: Lightly Unbalanced *MuB*: Moderately Unbalanced *HuB*: Highly Unbalanced

M2: Neutral-Equipped MPSDP-Based OPF Relaxation

variable : $\hat{\mathbf{W}}$

subject to :

$$\mathrm{Tr}(\hat{\Psi}^{\varphi}_{k,nw_{p/q}}\hat{\mathbf{W}}) + P^{\varphi}_{k,gnd}/Q^{\varphi}_{k,gnd} + P^{\varphi}_{k,l_{inj}}/Q^{\varphi}_{k,l_{inj}} = 0, \quad \forall\varphi \in \phi_k, k \in N \setminus G \tag{35a}$$

$$\underline{P}_{g_i}/\underline{Q}_{g_i} \leq \mathrm{Tr}(\hat{\Psi}^{\varphi}_{i,nw_{p/q}}\hat{\mathbf{W}}) + P^{\varphi}_{i,gnd}/Q^{\varphi}_{i,gnd} + P^{\varphi}_{i,l_{inj}}/Q^{\varphi}_{i,l_{inj}} \leq \overline{P}_{g_i}/\overline{Q}_{g_i}, \quad \forall\varphi \in \phi_i, i \in G \tag{35b}$$

$$|\underline{V}_k|^2 \leq \mathrm{Tr}(\hat{\Psi}^{\varphi}_{k,nw_v}\hat{\mathbf{W}}) \leq |\overline{V}_k|^2, \forall\varphi \in \eta_k, k \in N^+ \tag{35c}$$

$$\hat{\mathbf{W}} \succeq 0 \tag{35d}$$

$$\mathrm{rank}(\hat{\mathbf{W}}) = 1 \tag{35e}$$

complete ZIP load become:

$$P^{\varphi}_{k,l_{inj}} = \mathrm{Tr}(\hat{\Psi}^{\varphi:Z\%}_{k,l_p}\hat{\mathbf{W}}) + \mathrm{Tr}(\hat{\Psi}^{\varphi:P_c\%}_{k,l_p}\hat{\mathbf{W}}) - \mathrm{Tr}(\hat{\Psi}^{\varphi:P\%}_{k,l_p}\hat{\mathbf{W}}) + \mathrm{Tr}(\hat{\Psi}^{\varphi:P\%}_{k,l_p}\hat{\mathbf{W}}_0) + \mathrm{Tr}(\hat{\Psi}^{\varphi:I_c\%}_{k,l_p}\hat{\mathbf{W}}) - \mathrm{Tr}(\hat{\Psi}^{\varphi:I\%}_{k,l_p}\hat{\mathbf{W}}) + P^{\varphi:I_{Abs}}_{k_{(r)}} \tag{36}$$

$$Q^{\varphi}_{k,l_{inj}} = \mathrm{Tr}(\hat{\Psi}^{\varphi:Z\%}_{k,l_q}\hat{\mathbf{W}}) + \mathrm{Tr}(\hat{\Psi}^{\varphi:P_c\%}_{k,l_q}\hat{\mathbf{W}}) - \mathrm{Tr}(\hat{\Psi}^{\varphi:P\%}_{k,l_q}\hat{\mathbf{W}}) + \mathrm{Tr}(\hat{\Psi}^{\varphi:P\%}_{k,l_q}\hat{\mathbf{W}}_0) + \mathrm{Tr}(\hat{\Psi}^{\varphi:I_c\%}_{k,l_q}\hat{\mathbf{W}}) - \mathrm{Tr}(\hat{\Psi}^{\varphi:I\%}_{k,l_q}\hat{\mathbf{W}}) + Q^{\varphi:I_{Abs}}_{k_{(r)}} \tag{37}$$

which can be combined with (34a)-(34b) to express the multi-phase OPF model for DNNs as shown in **M2**. Please note that this model is still a non-convex model but the non-convexity is constrained in (35e) which can be dropped to obtain a convexified OPF model.

VI. NUMERICAL TESTS

In this section, the quality of proposed MPSDP-based OPF relaxation **M2** in terms of recovered solution and CT is reported for several combinations of ZIP load parameters and grounding impedance values. The proposed relaxation is applied on several MV (IEEE-13 [40], MG [29]) and LV (CIGRE [41], IT-37 [42] & IT-111 [39]) active DNs with their degree of unbalance as mentioned in Table 1. For all simulation scenarios, $\underline{V}$ and $\overline{V}$ are set to 0.90 and 1.05 pu, respectively. The simulations are carried out using a MATLAB-based tool box YALMIP [43] along with MOSEK solver on a DELL 64-bit OS, core i7 with a processor speed of 2.80 GHz and 16 GB RAM.

A. CRITERIA FOR THE NUMERICAL EXACTNESS

Three metrics namely Eigen Value Ratio (EVR) [32], [44], power mismatch at load (PQ) buses [26] and Cumulative Normalized Constraint Violation (CNCV) [45] are used to check the optimality and feasibility of the recovered solution provided by the proposed relaxation for several combinations of Load Models (LMs) [46].

The EVR is defined as the ratio between the two largest eigenvalues of the obtained solution ($\hat{\lambda}_P$ and $\hat{\lambda}_{P-1}$) which are recovered from the Hermitian matrix $\hat{\mathbf{W}}$ having dimensions equal to $P = n \times \tau + 1$. Ideally, all eigenvalues except one of this matrix should be zero if its recovered rank is 1. However, due to the limited numerical precision of SDP solvers, it is not possible to satisfy the rank-1 condition (35e) even

though the relaxed problem is exact. The EVR is calculated as $|\hat{\lambda}_{P-1}|/|\hat{\lambda}_P|$ where $|\hat{\lambda}_{P-1}|/|\hat{\lambda}_P| \geq 0$ and the obtained solution is considered as a rank-1 solution for $|\hat{\lambda}_{P-1}|/|\hat{\lambda}_P| \leq 10^{-5}$. It is important to mention that %Optimality Gap (OG) is another metric [16], [47] which is normally used to check the difference between the objective values of a relaxation and its non-convex model which is normally solved by a non-linear solver such as IPOPT [48] etc. However, in this work, several open source non-convex solvers such as IPOPT [48], FMINCON, FilterSD [49] and SNOPT [50] failed to solve the multi-phase non-convex OPF model. Consequently, the %OG metric is not used to check the optimality of the obtained solution.

Due to the heuristic nature of EVR criterion (selection of 10^{-5} is user dependent) and the inability of implementing %OG metric, power mismatch and CNCV metrics are utilized as additional criteria to check the feasibility of proposed relaxation. The power mismatch criterion checks the power balance constraint at each load bus once the relaxation is solved. In case of a feasible recovered solution, *ideally* the active and reactive power mismatch at each load bus must be zero. However, numerically it is not possible and, therefore, in this work, the threshold value for power mismatch criterion is selected as 10^{-2} [W/VAr] which is lower than the usually specified tolerance value of 10^{-1} in power flow solution packages such as PSS/E, and any recovered solution which violates this threshold at any of the load buses is considered as a suboptimal (rank-2) or a completely meaning less (higher than rank-2) solution.

In CNCV criterion, the distance to AC feasibility is calculated if convex relaxation provides an infeasible solution. For this purpose, a simple power flow is run by setting the *initial voltages* at network buses and *active/reactive power set-points* of DGs equal to the values obtained from the *infeasible* solution and after obtaining the feasible solution from power flow, the following CNCV parameter is determined.

$$x_{viol} = \sum_{k \in X} \frac{max(x_k^{AC-PF} - \overline{x}_k, \underline{x}_k - x_k^{AC-PF}, 0)}{\overline{x}_k - \underline{x}_k} \times 100\% \quad (38)$$

where $x = \{P_g^{\varphi}, Q_g^{\varphi}, |V^{\varphi}|\}$ and $X = \{G, G, N\}$. However, in this work, this criterion is slightly modified by replacing the state variables values obtained from the power flow (x_k^{AC-PF}) with the state variables values obtained from the OPF relaxation ($x_k^{OPF-Rlx}$) to determine if the voltage at any phase of a node and active/reactive power set-points of DGs have violated the constraints (35c), and (35b), respectively. A cumulative value of 0 indicates that a state variable has not violated its FR and, therefore, the obtained optimal value is a feasible one. In the case of non-zero cumulative value, (38) can, subsequently, be used to determine the distance of state variables to the feasibility point.

Finally, the Objective Functions (OFs) considered in this paper are the minimization of slack bus power (OF1) and minimization of active power losses (OF2).

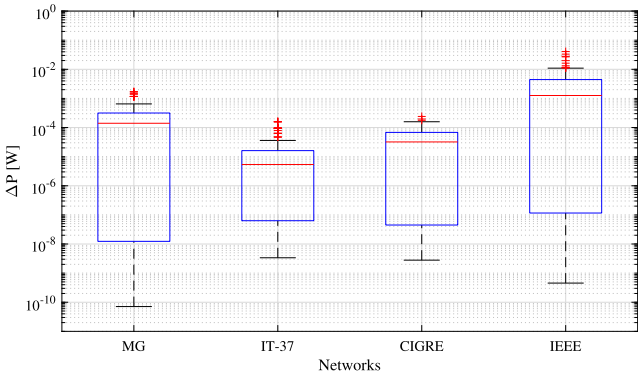

FIGURE 3. Active power mismatch at all load buses under all LMs for OF2.

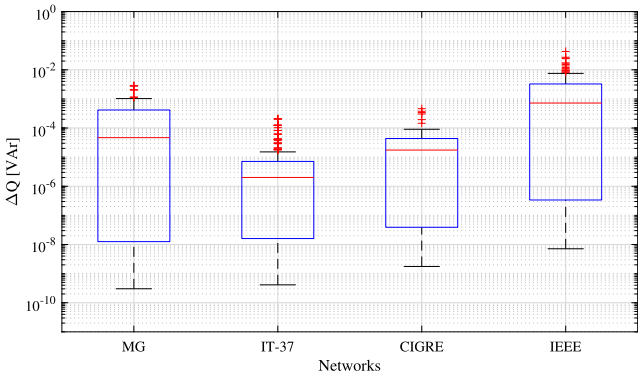

FIGURE 4. Reactive power mismatch at all load buses under all LMs for OF2.

B. QUALITY ASSESSMENT OF THE PROPOSED OPF RELAXATION

Table 1 summarizes the results related to the exactness and computational efficiency of the proposed scheme. Figs. 3 and 4 represent the active and reactive power mismatch at all load buses and Fig. 5 shows the voltages at all phases of the test networks when **M2** is solved for all LMs. The following key observations can be noted from the obtained results.

- For all LMs which are independent of constant current component, an exact solution is obtained for all DNs irrespective of their degree of unbalance.
- For lightly and moderately unbalanced DNs, the proposed relaxation is tight, i.e., $|\lambda_{P-1}|/|\lambda_P| \leq 10^{-5}$, for both OFs under various combinations of realistic LMs involving constant current components.
- In the case of highly unbalanced DNs, a higher EVR is obtained under the scenario when constant current component dominates the other components in terms of power injections as can be noticed for LMs 4 and 6. This is caused by the approximate modelling of this component since imaginary part of phases voltages cannot be ignored under highly unbalanced grid operation. Consequently, with respect to the EVR criterion, the relaxation becomes inexact and provides a suboptimal solution.

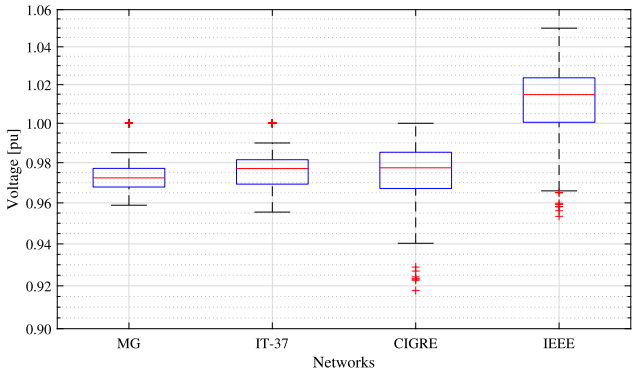

FIGURE 5. Phases voltage under all LMs for all the test networks for OF2.

- In terms of power mismatch and CNCV criteria, the *apparent* exactness of proposed relaxation in the case of lightly and moderately unbalanced DNs, as perceived by the satisfaction of EVR criterion, is further supported by the non-violation of these metrics for all LMs. Resultantly, the obtained solution is regarded as an optimal and feasible solution. On the other hand, for highly unbalanced IEEE-13 bus network, a higher EVR is obtained in the case of LMs 4 and 6 which makes the relaxation inexact and, consequently, as per expectation, the active and reactive power mismatch values for these LMs have also violated the specified threshold level as can be noticed by the extreme outliers in Figs. 3-4 which indicate that the constraint (35a) is weakly satisfied at load buses. However, in the case of CNCV criterion, a value of 0 is obtained for all test cases. Since this criterion is satisfied for all LMs and DNs, it is, therefore, pointless to represent a table showing 0 values for all the state variables. Instead voltage feasibility is presented in Fig. 5 which clearly shows that the recovered voltages at all nodes remain within the prescribed voltage limits. The obtained value of CNCV criterion *apparently* contradicts the results obtained from the EVR and power mismatch criteria in this sense that one should also expect the network voltages, in the case of LMs 4 and 6, to violate the voltage FR. However, this is not the case due to the fact that initial voltages are set to 1.05pu at all buses in this case, rather than 1.0pu as per the given IEEE data sheet, and this allows the voltages at all buses to stay above the lower limit value.[1] Consequently, the obtained solution, although remains feasible with respect to the voltage values, is considered as a suboptimal solution due to the violation of EVR and power mismatch criteria.
- For CIGRE DN which is also highly unbalanced, a high EVR is obtained in the case of OF1 for LM 4. However, both power mismatch and CNCV criteria are satisfied in this case (graphs are not shown here) which indicates that the obtained solution, which indeed satisfies the power balance equalities at all load buses as well as the voltage constraints at all network buses but has an EVR very close to 10^{-4}, can be considered as rank-1 solution. Resultantly, it is justified to say that the chosen EVR criterion is quite stringent in terms of characterizing the obtained solution as a rank-1 or higher than rank-1 solution.
- With respect to the highly unbalanced DNs, all evaluation criteria are satisfied in the case of LMs having lower contribution from the constant current load and, therefore, the obtained solution is considered exact for all such cases.
- An interesting observation can be made about the median value of power mismatch criterion which starts increasing with an increase in the degree of unbalance i.e., from IT-37 to IEEE-13. In the case of IT-37 and CIGRE DNs, which are relatively less unbalanced in comparison to the IEEE-13 network, the median value of both active and reactive mismatch remains within $10^{-6} - 10^{-4}$ [W/VAr] range, whereas in the case of IEEE-13 bus network, the median value stays between $10^{-4} - 10^{-3}$ [W/VAr] range. Consequently, it is perceivable that a higher rank solution can be obtained for a highly unbalanced DN particularly if it is serving a large load of constant current type. However, the same trend is not observed for the lightly unbalanced MG DN which represents a higher median value of power mismatch as compared to the values obtained in the case of IT-37 and CIGRE DNs. This is due to the fact that some branches/lines of this network are extremely short and, as a result, the poor numerical data in the admittance matrix (high admittance values related to these lines) of this network causes the solver to provide an inferior solution.
- For IT-111 bus system, MOSEK is unable to solve the developed OPF relaxation due to the large dimensions of $\hat{\mathbf{W}}$ which, in turn, leads to the formation of extremely large number of internally generated constraints ($\sim$130k) and causes the solver to hit its memory limit. Consequently, for this network, a cheap conic SDP-based OPF relaxation termed as BFM-based SDP relaxation is solved. Please note that the proposed MPSDP-based OPF relaxation generalizes (more tighter) the cheap conic SDP-based OPF relaxation even in the case of radial DNs unless an equivalence is established between them for this network type. Despite being weaker, an exact solution is obtained for this test network in all cases through the cheap conic relaxation as evident by the results shown in Table 1 which indicate that the proposed MPSDP-based OPF relaxation will definitely provide an exact solution with the emergence of more stable and advanced SDP solvers.
- It must be noted that other SDP solvers such as SeDuMi [51], CSDP [49], DSDP [49] and SDPT3 [52]

[1]The initial voltage level is set to 1.05pu due to the fact that network is heavily loaded and setting an initial value equal to 1.0pu causes the voltage to violate the lower limit even in the case of a simple power flow study. Therefore, in order to obtain a feasible solution, the voltages on secondary side of RG60 are raised to 1.05pu.

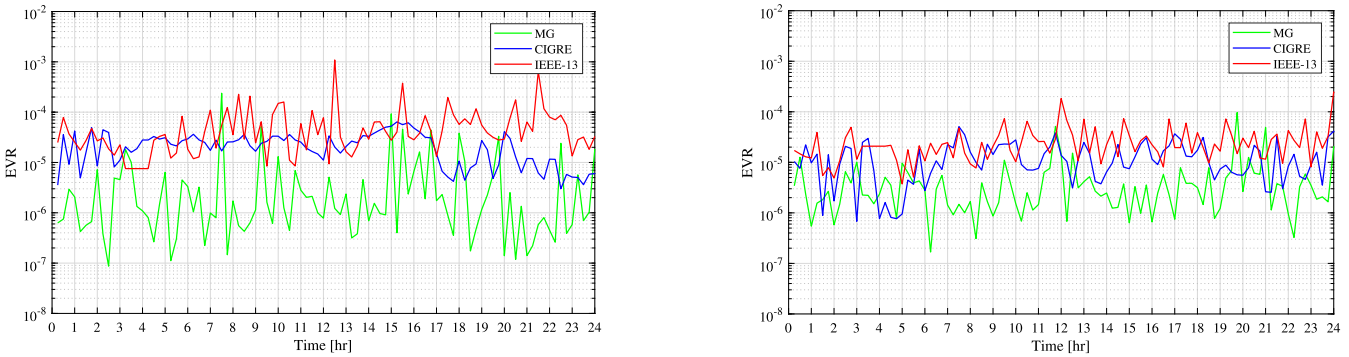

FIGURE 6. Impact of end-users profiles on EVR for LM 4 (a) both load and generation profiles are time varying (b) time varying load and rated (fixed) generation profiles.

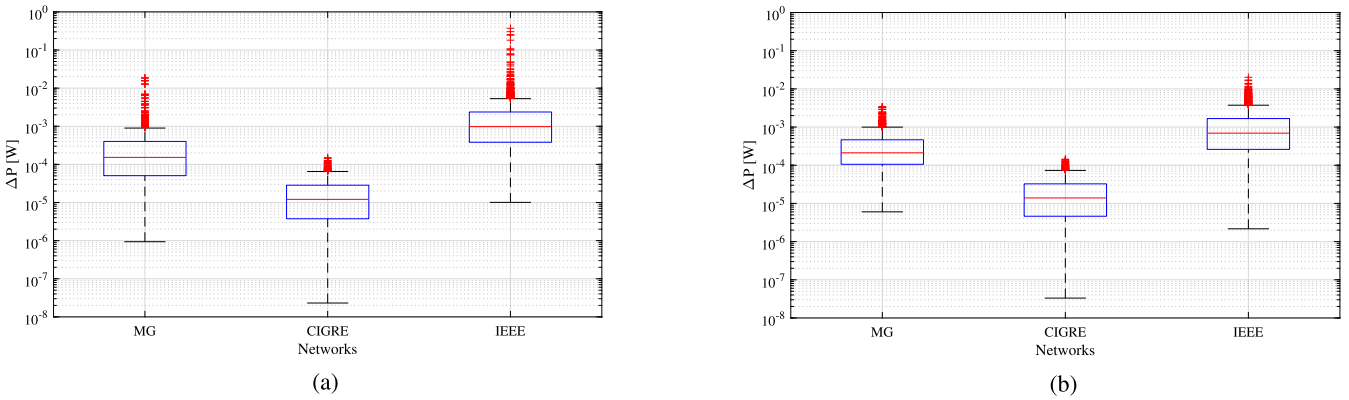

FIGURE 7. Impact of end-users profiles on active power mismatch for LM 4 (a) both load and generation profiles are time varying (b) time varying load and rated (fixed) generation profiles.

have also been utilized to solve the model **M2** but all of them reported either numerical problem or produced sub-optimal results. It is expected that with the emergence/improvement of SDP solvers, a higher EVR and, consequently, a more accurate solution will be obtained, but as per authors knowledge, MOSEK is the most widely used solver for SDP problems because of its reliability (even in the case of poor numerical data) and high computational efficiency.

C. EXACTNESS OF THE PROPOSED RELAXATION UNDER TIME VARYING LOADS AND DG PROFILES

In the previous section, the exactness of MPSDP-based OPF relaxation is tested under extreme loading conditions i.e., rated load and generation profiles are used which put maximum stress on DNs. However, in real-time load profiles rarely touch their peak levels and remain well below their rated level. Resultantly, a more realistic case study is presented in this section to evaluate the exactness of proposed relaxation under two LMs 4 and 5 for time-varying loads and DGs profiles. The chosen LMs represent two extremes in terms of contribution from the constant current load. For each LM, the following two case studies are carried out.

Case-1: Time varying loads and DGs profiles
Case-2: Time varying loads and rated DGs profiles

The simulations are carried out for one day and the same three criteria, as reported in the previous section, are utilized for the evaluation of both case studies. Figs. 6-9 show the results for LM 4 whereas Figs. 10-13 show the results for LM 5. The following observations can be made from the obtained results.

- With respect to the case study 1 and LM 4, the relaxation appears to be exact for CIGRE DN as evident by the satisfaction of all criteria i.e., the EVR is less than 1×10^{-4}, the extreme outliers in the case of power mismatch remain well below the specified threshold value and recovered voltages at all nodes stay within the FR over the whole simulation period as can be noticed in Figs. 6a-9a. In the case of MG DN, the relaxation remains exact over the complete simulation range except at one time instant [7-1/2$^{\text{th}}$]hr where EVR goes slightly above its threshold level and power mismatch criterion is weakly violated as well. However, phases voltages remain within the defined FR even in this case and no violation of CNCV criterion is observed at any time instant. Consequently, the obtained solution, although

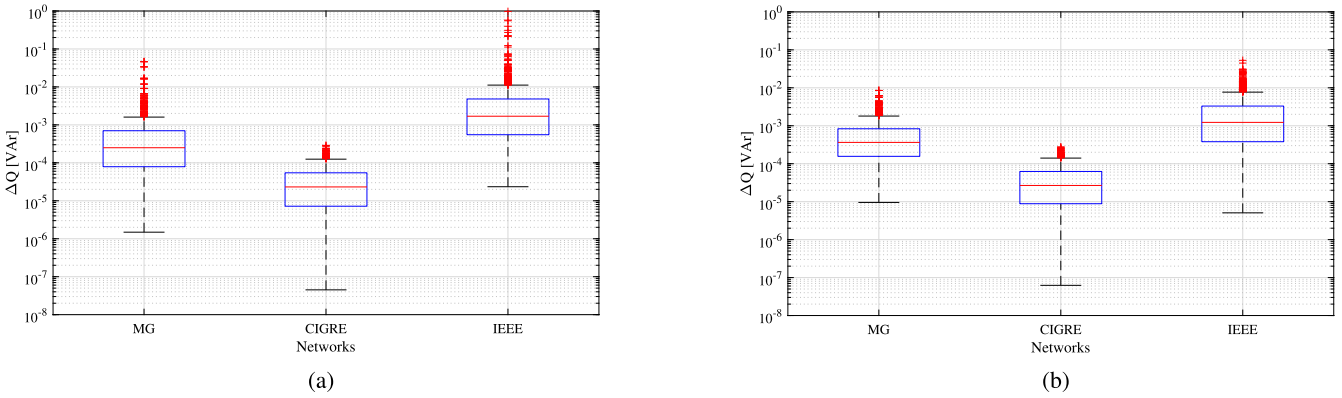

FIGURE 8. Impact of end-users profiles on reactive power mismatch for LM 4 (a) both load and generation profiles are time varying (b) time varying load and rated (fixed) generation profiles.

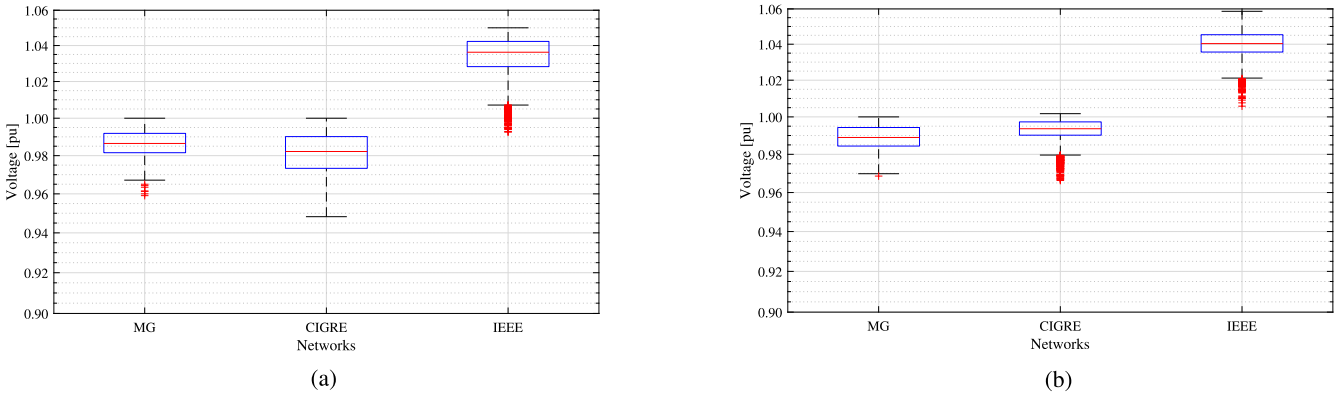

FIGURE 9. Impact of end-users profiles on recovered voltages for LM 4 (a) both load and generation profiles are time varying (b) time varying load and rated (fixed) generation profiles.

a suboptimal solution, can be used as an initial input to a non-linear global solver due to the fact that the probability of the existence of a global solution in the vicinity of the obtained solution is very high. In the case of IEEE-13 node network, it was expected that the relaxation would provide a suboptimal solution due to its highly unbalanced nature. However, it can be noticed that it remains exact over a large number of time instants and inexactness is observed only at those instants when system loading becomes too high without enough output from the local DGs. Consequently, the EVR criterion is violated as well as the active and reactive power mismatch values become 10^0 in the case of extreme outliers. These results further confirm the previously reported findings that in the presence of dominant constant current injections, a highly unbalanced DN can lead to a poor and suboptimal OPF solution if it is heavily loaded. On the other hand, the same network has the tendency to provide an exact solution for the same type of LMs if it is lightly or moderately loaded. On the other hand, lightly and moderately unbalanced DNs can provide an exact solution irrespective of the injections magnitude from constant current load.

- With respect to the case study 2 and LM 4, it can be noticed in Fig. 6b that the EVR has improved for all DNs and, in particular, only two violations are observed for IEEE-13 bus network whereas no violation is noted for MG and CIGRE DNs. Furthermore, both active and reactive power mismatch criteria are satisfied for the latter networks and a significant improvement regarding satisfaction of mismatch criterion is achieved for the former network as can be noted by the reduced median value and lower value of extreme outliers. Similarly, the median value of recovered voltages has also increased for all DNs and the values of 25^{th} and 75^{th} percentiles are now more close to the median value, therefore indicating a more balanced grid. These findings indicate that the proposed relaxation has tightened as compared to the case study 1 which involves both time-varying load and DG profiles.
- The previous discussion shows that MPSDP-based relaxation has the tendency to remain exact under realistic time-varying loads and rated DGs profiles in the case of those largely dominated constant current LMs which exhibit inexactness under extreme network loading scenario.

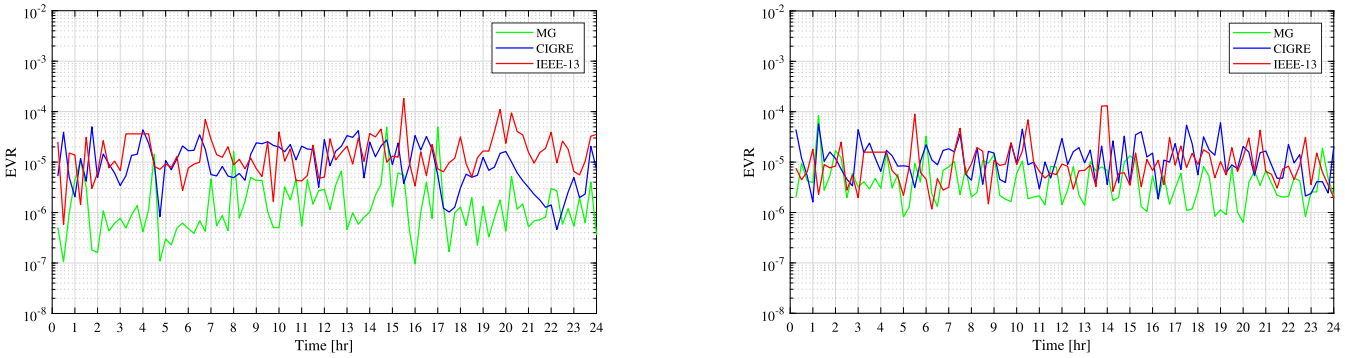

FIGURE 10. Impact of end-users profiles on EVR for LM 5 (a) both load and generation profiles are time varying (b) time varying load and rated (fixed) generation profiles.

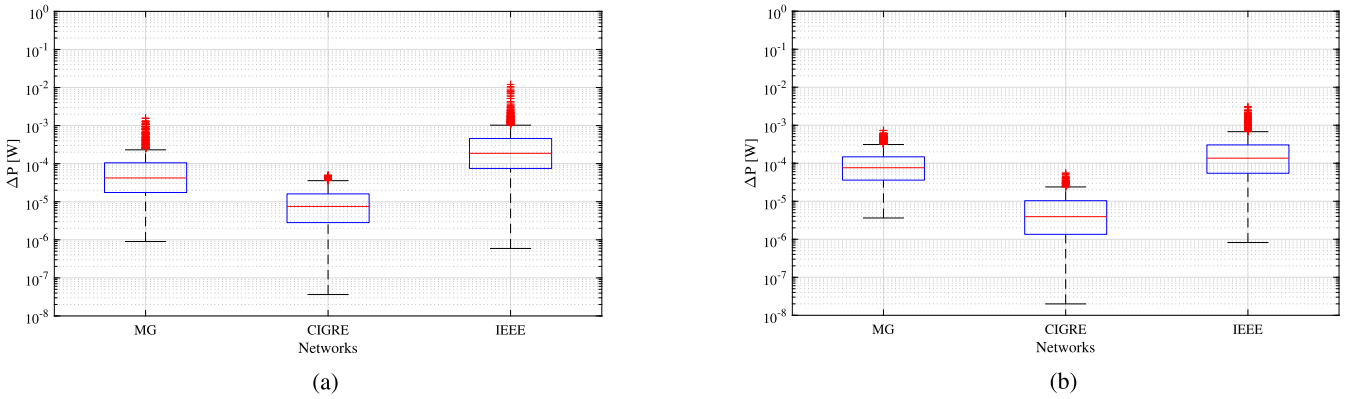

FIGURE 11. Impact of end-users profiles on active power mismatch for LM 5 (a) both load and generation profiles are time varying (b) time varying load and rated (fixed) generation profiles.

- With respect to LM 5, it can be noticed in Figs. 10-13 that under mild contribution from the constant current load, the relaxation provides an exact solution for both MG and CIGRE DNs in both case studies as evident from the satisfaction of all three criteria.
- In the case of IEEE-13 node DN, it is expected that the relaxation would remain exact under both time-varying and rated DG profiles since the connected ZIP load has dominant constant impedance and constant power components. However, a higher value of EVR is observed at one time instant in both cases which indicates that the obtained solution is a higher rank solution. However, a closer look at the active and reactive power mismatch values show that only few outliers are above or equal to the threshold level in the first case (Fig. 11a-12a) whereas no violation of power mismatch criterion is observed in the second case (Fig. 11b-12b). Furthermore, in both case studies, the power mismatch values remain well below the specified threshold level for all the other time instants. Moreover, the CNCV criterion is satisfied as well throughout the simulation range for both test scenarios. Consequently, it can be expected under moderate contribution from constant current loads, an exact solution can be obtained for highly unbalanced DNs.
- Finally, to conclude the above-mentioned discussion about the exactness, and lack-thereof, of proposed relaxation with respect to the degree of unbalance and constant current load injections, an explicit case study is shown in Fig. 14 solely for MG DN, which represents the impact of increasing unbalance in the presence of LM 4. It can be noticed that by going from lightly unbalanced case to highly unbalanced scenario, all evaluation criteria starts reaching their specified threshold levels. The average value of EVR criterion increases significantly from the lightly unbalanced case to the highly unbalanced scenario and relaxation even becomes inexact for the latter case at one time instant. Similarly, the median value of power mismatch criterion has also increased along with the emergence of more extreme outliers. The same behaviour is also noted for the phases-voltages values. Resultantly, it can be concluded that under realistic time-varying load profiles, the relaxation provides an exact solution irrespective of the degree of unbalance in a network as long as injections from a constant current component and system loading do not become too large.

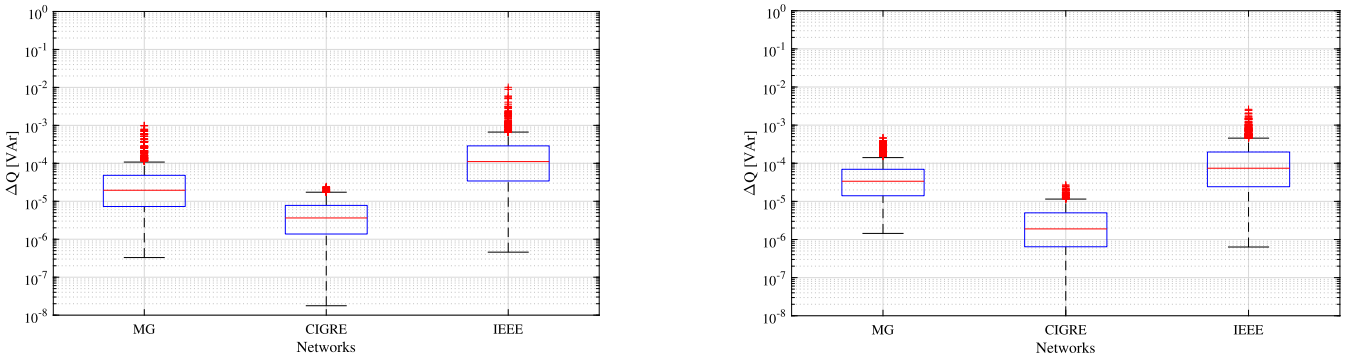

FIGURE 12. Impact of end-users profiles on reactive power mismatch for LM 5 (a) both load and generation profiles are time varying (b) time varying load and rated (fixed) generation profiles.

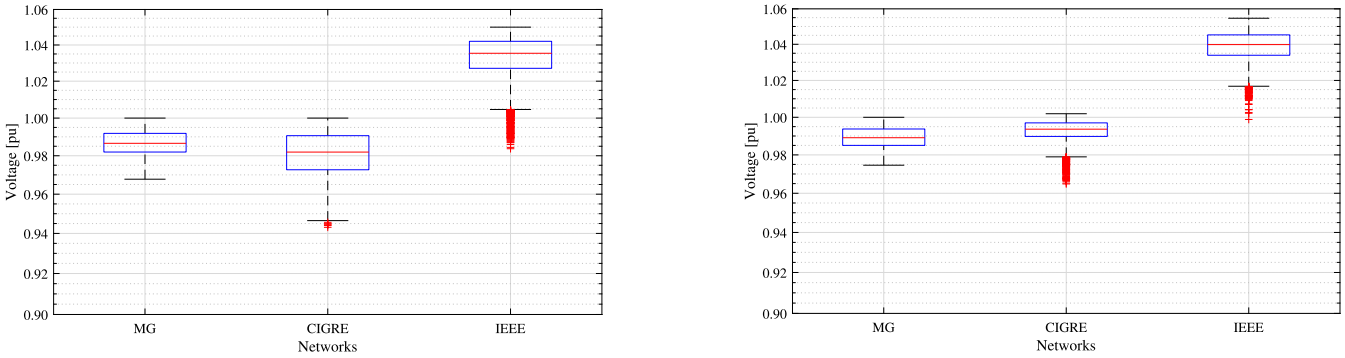

FIGURE 13. Impact of end-users profiles on recovered voltages for LM 5 (a) both load and generation profiles are time varying (b) time varying load and rated (fixed) generation profiles.

D. COMPUTATIONAL EFFICIENCY

The CT of proposed approach is shown in Fig. 15a and reported in Table 1 for each LM. It can be noticed that CT increases remarkably with an increase in network size as can be observed for IT-37 bus system. With such a large CT, the real-time implementation of MPSDP-based OPF relaxation for medium and large size DNs is practically non-viable. Moreover, it can also be noted that the CT increases significantly when the dimension of an OPF problem increases by one i.e., from 3-phase to 4-conductor system as shown in Fig. 15b. In the case of small DNs such as MG, CIGRE and IEEE, the CT increases almost by a factor of 3-4, whereas in the case of IT-37 bus network, a 6-7% increase in the time is observed.

The CT of IT-111 bus system cannot be compared with the CT of other networks due to the formation of OPF problem through the cheap conic relaxation methodology. However, it can be observed that this relaxation can practically be realized due to its low computational requirements, provided it computes the exact solution. The high CT associated with a large-scale SDP problem is a well known problem in the literature and several techniques based on sparsity exploitation [21], [25]–[27], [53] and distributed algorithms [29], [54]–[56] have been proposed for CT reduction which can, in turn, be adopted for medium and large size DNs to realize the real-time implementation of proposed relaxation for these networks.

E. IMPACT OF GROUNDING IMPEDANCE

The grounding impedance also has a strong impact on the quality of proposed relaxation as evident from the results, reported in Table 2, which are obtained by varying the grounding impedance from $1 \times 10^{-6}\Omega$ to $1 \times 10^{5}\Omega$ for MPG DNs and by setting it to $1 \times 10^{10}\Omega$ for SPG DNs under a fixed constant power LM. To evaluate the impact of grounding impedance, the objective value of MPSDP-based OPF relaxation is compared with the optimal value obtained from the KR-based OPF model through a %Relative Difference (RD) criterion as represented in (39). Please note that the **bold** values reported in the table represent the cases where all evaluation criteria are satisfied and %RD is greater than 1%.

$$\%\text{Relative Difference} = \frac{|obj_{MP} - obj_{KR}|}{obj_{MP}} \times 100 \quad (39)$$

The following key observations can be made with respect to the presented case study:

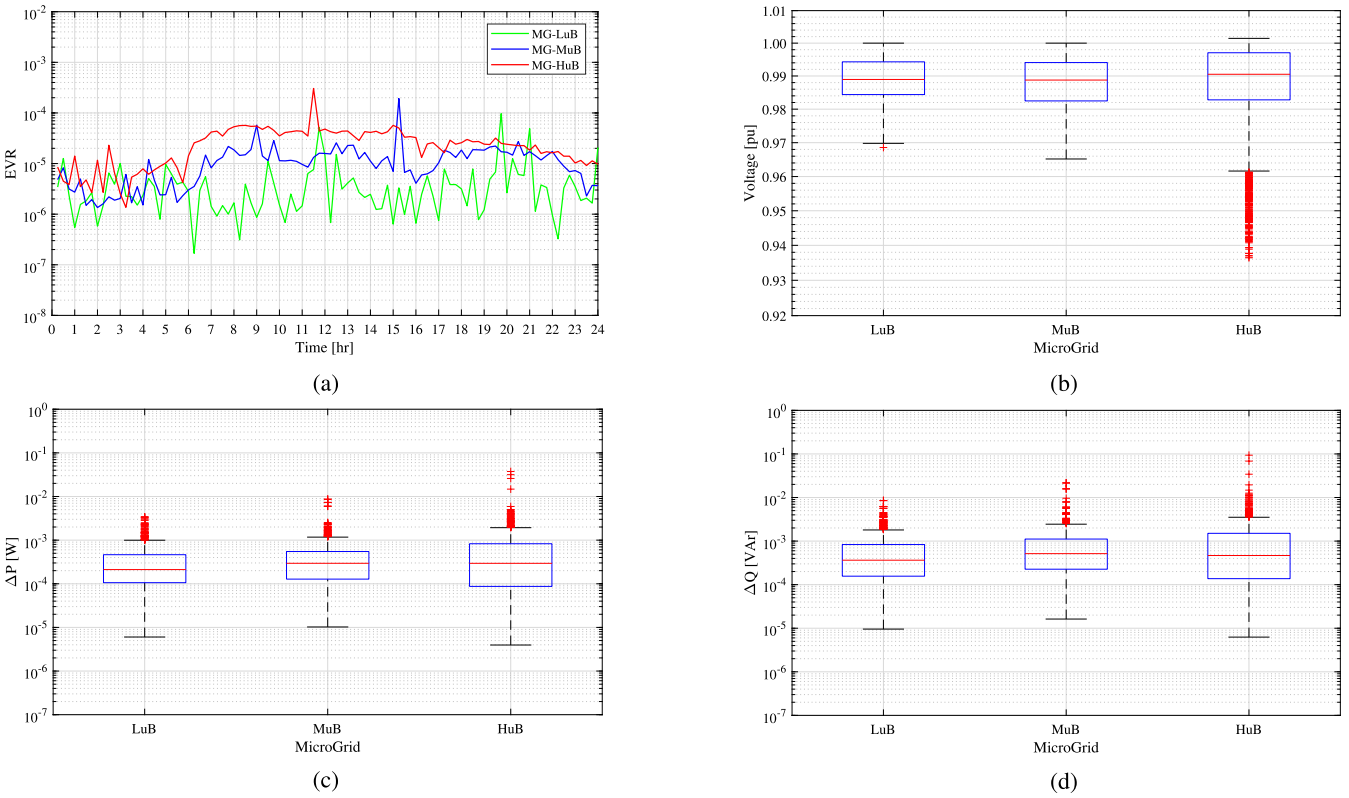

FIGURE 14. Impact of degree of unbalance on the quality of proposed relaxation when tested for LM 4 (a) EVR (b) recovered voltages (c) active power mismatch (d) reactive power mismatch.

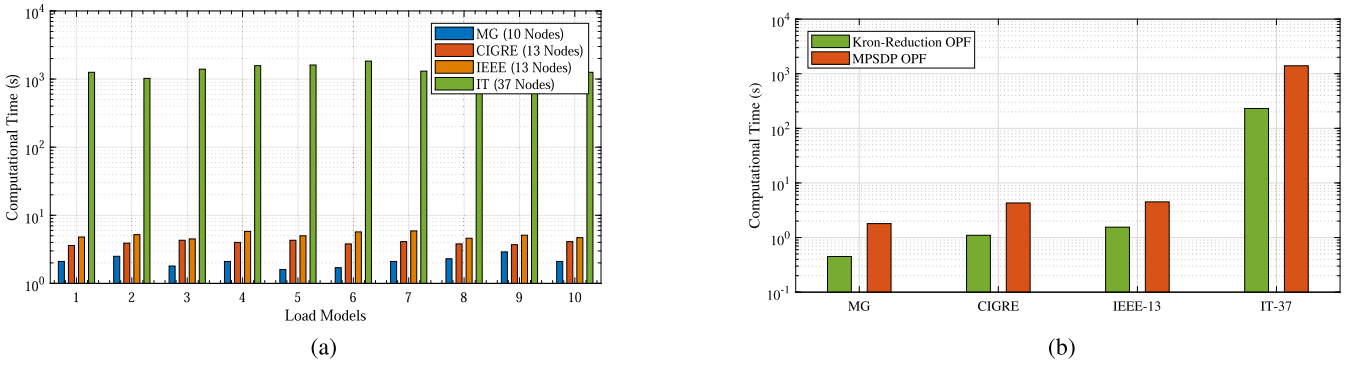

FIGURE 15. (a) Impact of increasing network size on the CT of proposed relaxation (b) Comparison of the CT of developed approach with the CT of KR-based OPF model.

- Emulating KR scenario by putting an extremely small value of grounding impedance leads to a high EVR as can be seen in the first three cases when proposed relaxation is solved for OF1. However, the same trend is not observed in the case of OF2 where a less than 1%RD is observed. Since OF1 deals with the apparent power injection at slack bus to which no load is attached, the grounding impedance value, as a result, becomes significantly relevant in this case. An extremely small value of it (e.g., $1 \times 10^{-6}\Omega$) sets the values of extreme (smallest and largest) coefficients in the OF polynomial equal to 6.8×10^{-13} and 5.3×10^{7}, respectively, whereas in the case of 1Ω value, these coefficients take the value 6.8×10^{-13} and 1.3×10^{4}, respectively. A significant reduction in the range of OF polynomial coefficients can be noticed with an increase in the value of grounding impedance, which, in turn, stabilises the input numerical data from the solver perspective and, as a result, a meaningful solution is obtained in the latter case. The presented results show that for DNNs, the proposed multi-phase relaxation can mimic an OPF model based on the KR approach, provided a SDP solver is capable of handling poor numerical data.

TABLE 2. Impact of grounding impedance on the quality of proposed scheme in comparison to the Kron-reduction based three-phase OPF model.

Grounding Impedance Ω	MG		IEEE-13		CIGRE		MG		IEEE-13		CIGRE	
	OF:1 Slack Bus Power (kVA)						OF:2 Network Losses (kW)					
	Three-Phase Kron Reduced Network						*Three-Phase Kron Reduced Network*					
	Value (kVA)	**Time** (s)	**Value** (kVA)	**Time** (s)	**Value** (kVA)	**Time** (s)	**Value** (kW)	**Time** (s)	**Value** (kW)	**Time** (s)	**Value** (kW)	**Time** (s)
	3048.7	0.43	4057.8	1.55	162.8	1.10	105.0	0.60	307.2	1.65	7.76	1.10
	Multi-Phase (Four Conductor) Network						*Multi-Phase (Four Conductor) Network*					
	Diff. %	**EVR** $\times 10^{-5}$	**Diff.** %	**EVR** $\times 10^{-5}$	**Diff.** %	**EVR** $\times 10^{-5}$	**Diff.** %	**EVR** $\times 10^{-5}$	**Diff.** %	**EVR** $\times 10^{-5}$	**Diff.** %	**EVR** $\times 10^{-5}$
1×10^{-6}	93.0	$> 10^4$	87.4	$> 10^4$	80.0	$> 10^4$	0.47	0.21	**1.38**	0.75	0.53	0.15
1×10^{-5}	90.2	$> 10^4$	86.4	$> 10^4$	6.91	66.3	0.14	1.06	**2.10**	0.52	**1.65**	0.25
1×10^{-4}	88.3	$> 10^4$	76.6	$> 10^4$	0.49	1.38	0.24	0.05	**2.46**	0.45	**2.82**	0.04
1×10^{-3}	3.30	12.3	11.5	79.4	0.54	2.03	0.29	0.26	**4.66**	5.10	**3.49**	0.26
1×10^{-2}	0.12	1.35	0.50	5.10	0.57	4.00	0.41	0.06	**3.65**	2.50	**2.96**	0.01
1	0.91	0.16	**2.56**	1.50	**2.26**	0.72	**2.07**	0.25	**9.67**	0.36	**1.42**	0.42
5	0.31	0.04	**1.11**	5.30	**1.15**	4.50	**2.08**	1.50	**3.78**	15.5	**3.38**	1.77
10	0.60	1.60	**1.40**	21.3	**1.16**	1.75	**2.33**	3.35	45.4	***22.3***	**3.33**	3.36
1×10^{2}	0.81	3.70	**1.21**	13.1	**1.18**	2.05	**2.52**	1.93	42.3	***26.2***	**3.87**	2.99
1×10^{5}	**1.32**	7.40	1.69	***47.1***	**1.13**	3.02	**3.40**	1.18	10.1	***19.7***	**3.10**	2.25
SPG	**1.47**	2.79	**1.94**	6.14	**3.27**	***15.6***	**2.44**	0.08	**11.7**	9.80	**9.16**	***13.4***

- With the increase in grounding impedance value from $1 \times 10^{-2}\Omega$ to $1 \times 10^{5}\Omega$, the %RD starts to increase due to the rise in neutral current, and consequently, the values of OFs, particularly network losses, start deviating significantly from the values obtained from the Kron-reduced network since in such DN, the current tends to flow through the ground rather than taking the neutral conductor path. It can be noticed that in the case of OF1, the %RD is as large as 2% whereas in the case of OF2, it has reached to 9%. Similarly, in the case of SPG DN, an 11% RD is observed. These results suggest that the application of KR methodology on DNNs leads to suboptimal results and, therefore, its utilization on neutral-equipped DNs must be avoided.
- With an increase in the degree of unbalance, putting a high neutral-ground impedance to mimic an open circuit condition leads to a high rank solution as can be noticed in few cases (***bold-italic***) of IEEE-13 node and CIGRE DNs. In all such cases, all three evaluation criteria are violated.

The above-mentioned observations demonstrate that the different values of grounding impedance lead to the objective values which can differ significantly from the results obtained from the KR-based OPF model. Consequently, it is unrealistic to adopt this approach for DNs in a which neutral conductor is either ungrounded or grounded through a finite resistance at a single or multiple points.

F. THEORETICAL GUARANTEE OF MULTI-PHASE SDP-BASED OPF RELAXATION

The proposed relaxation is also tested for other LMs (not reported here) which consist of large k_I values and it has been found that in majority of the cases, a high rank solution is obtained. Although, there exists some rank-recovery methods as reported in [13], [57], [58], these methods have only been tested for single-phase equivalent networks. Since the non-convexity of a multi-phase OPF problem is much stronger than the non-convexity of a single-phase OPF problem, the ability of these methods to recover a rank-1 solution in the case of an unbalanced multi-phase OPF problem is still an open research task. On the other hand, in the case of greater than rank-2 solution, the obtained solution has no physical meaning and the feasible solution cannot be recovered. In such a case, the obtained solution can be utilized as an input to a deterministic or heuristic algorithm (warm start) to obtain a feasible solution. Furthermore, there does not exist any theoretical guarantee (sufficient conditions) for the exactness of MPSDP-based OPF relaxation due to the extremely complex analytical characterization of power injections which represent strong mutual coupling among line power flows. In [29] and [33], some attempts are made to exhibit the FR of a two-bus three-phase network. For a strictly increasing OF with respect to the power injections, the FRs of non-convex AC-OPF and relaxed problems are shown to coincide with each other in [29] and, resultantly, it is expected that a rank-1 solution can be obtained for a three-phase unbalanced OPF problem. However, a counter example is provided in [33] which shows that the FR of the relaxed problem of the same network can become greater than the FR of the non-convex AC-OPF problem under a non-increasing OF and, therefore, the obtained solution can have a higher rank. These two counter examples clearly indicate that there is a strong need to develop sufficient condition(s) which can guarantee the exactness, and lack thereof, of a MPSDP-based OPF relaxation.

G. CONCLUDING REMARKS

To summarize the findings regarding the quality of proposed relaxation with respect to the degree of unbalance, contribution of ZIP load components, grounding impedance value and CT, a brief discussion is carried out in this section.

- In the case of solely Z, I or P loads, the relaxation recovers an exact solution under any degree of unbalance in a DN.
- In the case of ZIP loads, the relaxation provides an exact solution for lightly and moderately unbalanced DNs for all LMs as evident by the satisfaction of all three criteria. However, in the case of highly unbalanced DNs, the contribution of constant current load plays a significant role in the exactness of proposed relaxation which remains exact under low and moderate contribution from this load component. However, in the case of dominant injections from this load component, a higher EVR is obtained in the case of rated loading scenario as per expectation along with the weak satisfaction of power mismatch and CNCV criteria.
- The proposed relaxation provides an exact solution in the presence of realistic time-varying loads and DGs profiles i.e., in a realistic loading scenario, an optimal solution can be obtained even for LMs having large contributions from constant current loads and DNs exhibiting a high degree of unbalance.
- The KR methodology, when applied to MPG and SPG DNs, leads to an optimal value which differs significantly from the optimal value obtained from the MPSDP-based OPF relaxation. The grounding impedance, chosen OF and varying parameters of a ZIP load strongly impact the optimal solution value. However, under KR approach, the impact of these characteristics are lost completely. Consequently, the obtained solution from the KR-based OPF relaxation should be considered as a suboptimal solution.
- The CT of proposed relaxation increases to such an extent for a real DN, containing moderate number of nodes, that its real-time implementation cannot be practically realized unless additional strategies such as sparsity exploitation and/or distributed OPF algorithms are exploited for such networks.

VII. CONCLUSION

The coupled power injections across the conductors of neutral-equipped DNs are considered as the main bottleneck in the development of a convex OPF model for such networks. The proposed network admittance matrix-based methodology facilitates the decoupling of coupled power injections and provides explicit formulation of these injections for each phase and neutral conductor which ultimately leads to the development of a centralized SDP-based OPF model for DNNs. The novel complex voltage variable-based methodology overcomes the limitations of existing voltage magnitude-based approach for the modelling of a ZIP load in terms of optimization variable and, resultantly, allows to incorporate it in the proposed multi-phase relaxation without introducing new variables for each load bus.

The quality of proposed relaxation, as indicated by the EVR, power mismatch and CNCV criteria, is quite evident since it provides an exact solution irrespective of the degree of unbalance and contribution in terms of power injections from constant impedance and constant power components. Regarding injections from the constant current component, the relaxation remains exact for lightly and moderately unbalanced DNs under both realistic (time varying) and extreme (rated) loading cases irrespective of the magnitude of injection from this component. On the other hand, in the case of highly unbalanced DNs, the relaxation can provide a suboptimal solution for load models having dominated constant current component under heavily loaded conditions, whereas under realistic loading scenario, it has shown the tendency to provide an exact solution for all load models in such networks.

The grounding impedance value plays a significant role in the exactness of proposed relaxation as putting an extremely small impedance to mimic a solidly grounded configuration can lead to a higher rank solution because of the optimization solver inability to handle poor numerical input data. Furthermore, the unrealistic application of KR approach to SPG and MPG DNs provides an under/over estimated optimal solution as compared to the solidly grounded DNs and, therefore, it is practically non-viable to utilize this approach for DNs which are grounded either at single or multiple points through a finite impedance.

The computational requirement of the proposed relaxation for medium and large size DNs increases significantly in comparison to the computational time observed for the three-phase OPF model. Consequently, the real-time implementation of proposed approach seems hard to realize for such networks. To overcome this limitation, the work is in progress to develop a novel distributed algorithm with special emphasis on incorporating the proposed OPF relaxation in LV distribution management system for effective and optimal participation of DGs in the context of grid management.

ACKNOWLEDGMENT

The authors would like to thank Levi Cases Institute for Energy Economics and Technology for supporting this project, and the anonymous reviewers for their helpful comments and suggestions.

REFERENCES

[1] M. Usman, M. Coppo, F. Bignucolo, and R. Turri, "Losses management strategies in active distribution networks: A review," *Electr. Power Syst. Res.*, vol. 163, pp. 116–132, Oct. 2018.
[2] R. Caldon, M. Coppo, and R. Turri, "Distributed voltage control strategy for LV networks with inverter-interfaced generators," *Electr. Power Syst. Res.*, vol. 107, pp. 85–92, Feb. 2014.
[3] J. Hu, M. Marinelli, M. Coppo, A. Zecchino, and H. W. Bindner, "Coordinated voltage control of a decoupled three-phase on-load tap changer transformer and photovoltaic inverters for managing unbalanced networks," *Electr. Power Syst. Res.*, vol. 131, pp. 264–274, Feb. 2016.

[4] M. Usman, M. Coppo, F. Bignucolo, R. Turri, and A. Cerretti, "Multi-phase losses allocation method for active distribution networks based on branch current decomposition," *IEEE Trans. Power Syst.*, vol. 34, no. 5, pp. 3605–3615, Sep. 2019.
[5] K. Lehmann, A. Grastien, and P. Van Hentenryck, "Ac-feasibility on tree networks is NP-hard," *IEEE Trans. Power Syst.*, vol. 31, no. 1, pp. 798–801, Mar. 2015.
[6] H. W. Dommel and W. F. Tinney, "Optimal power flow solutions," *IEEE Trans. Power App. Syst.*, vol. PAS-87, no. 10, pp. 1866–1876, Oct. 1968.
[7] O. Alsac and B. Stott, "Optimal load flow with steady-state security," *IEEE Trans. Power App. Syst.*, vol. PAS-93, no. 3, pp. 745–751, May 1974.
[8] G. C. Contaxis, C. Delkis, and G. Korres, "Decoupled optimal load flow using linear or quadratic programming," *IEEE Trans. Power Syst.*, vol. PWRS-1, no. 2, pp. 1–7, May 1986.
[9] B. Ghaddar, J. Marecek, and M. Mevissen, "Optimal power flow as a polynomial optimization problem," *IEEE Trans. Power Syst.*, vol. 31, no. 1, pp. 539–546, Jan. 2016.
[10] I. M. Nejdawi, K. A. Clements, and P. W. Davis, "An efficient interior point method for sequential quadratic programming based optimal power flow," *IEEE Trans. Power Syst.*, vol. 15, no. 4, pp. 1179–1183, Nov. 2000.
[11] P. E. O. Yumbla, J. M. Ramirez, and C. A. C. Coello, "Optimal power flow subject to security constraints solved with a particle swarm optimizer," *IEEE Trans. Power Syst.*, vol. 23, no. 1, pp. 33–40, Jan. 2008.
[12] X. Bai, H. Wei, K. Fujisawa, and Y. Wang, "Semidefinite programming for optimal power flow problems," *Elect. Power Energy Syst.*, vol. 30, no. 6, pp. 383–392, Dec. 2008.
[13] J. Lavaei and S. H. Low, "Zero duality gap in optimal power flow problem," *IEEE Trans. Power Syst.*, vol. 27, no. 1, pp. 92–107, Feb. 2012.
[14] R. A. Jabr, "Radial distribution load flow using conic programming," *IEEE Trans. Power Syst.*, vol. 21, no. 3, pp. 1458–1459, Aug. 2006.
[15] M. Farivar and S. H. Low, "Branch flow model: Relaxations and convexification—Part I," *IEEE Trans. Power Syst.*, vol. 28, no. 3, pp. 2554–2564, Aug. 2013.
[16] C. Coffrin, H. L. Hijazi, P. V. Hentenryck, and C. E. Feb, "The QC relaxation : Theoretical and computational results on optimal power flow," *IEEE Trans. Power Syst.*, vol. 31, no. 4, pp. 3008–3018, Feb. 2016.
[17] W. Wei, J. Wang, N. Li, and S. Mei, "Optimal power flow of radial networks and its variations: A sequential convex optimization approach," *IEEE Trans. Smart Grid*, vol. 8, no. 6, pp. 2974–2987, Mar. 2017.
[18] C. Josz and D. K. Molzahn, "Moment/sum-of-squares hierarchy for complex polynomial optimization," 2015, *arXiv:1508.02068*. [Online]. Available: https://arxiv.org/abs/1508.02068
[19] J. Lavaei, D. Tse, and B. Zhang, "Geometry of power flows and optimization in distribution networks," *IEEE Trans. Power Syst.*, vol. 29, no. 2, pp. 572–583, Mar. 2014.
[20] B. Zhang and D. Tse, "Geometry of injection regions of power networks," *IEEE Trans. Power Syst.*, vol. 28, no. 2, pp. 788–797, May 2013.
[21] S. Sojoudi and J. Lavaei, "Physics of power networks makes hard optimization problems easy to solve," in *Proc. IEEE Power Energy Soc. General Meeting*, Jul. 2012, pp. 1–8.
[22] S. H. Low, "Convex relaxation of optimal power flow—Part I: Formulations and equivalence," *IEEE Trans. Control Netw. Syst.*, vol. 1, no. 1, pp. 15–27, Mar. 2014.
[23] L. Gan, N. Li, S. H. Low, and U. Topcu, "Exact convex relaxation of optimal power flow in radial networks," *IEEE Trans. Autom. Control*, vol. 60, no. 1, pp. 72–87, Jan. 2015.
[24] D. K. Molzahn and I. A. Hiskens, "A survey of relaxations and approximations of the power flow equations," *Found. Trends Electr. Energy Syst.*, vol. 4, nos. 1–2, pp. 1–221, 2018.
[25] R. A. Jabr, "Exploiting sparsity in SDP relaxations of the OPF problem," *IEEE Trans. Power Syst.*, vol. 27, no. 2, pp. 1138–1139, May 2012.
[26] D. K. Molzahn, J. T. Holzer, B. C. Lesieutre, and C. L. DeMarco, "Implementation of a large-scale optimal power flow solver based on semidefinite programming," *IEEE Trans. Power Syst.*, vol. 28, no. 4, pp. 3987–3998, Nov. 2013.
[27] M. S. Andersen, A. Hansson, and L. Vandenberghe, "Reduced-complexity semidefinite relaxations of optimal power flow problems," *IEEE Trans. Power Syst.*, vol. 29, no. 4, pp. 1855–1863, Jul. 2014.
[28] C. Bingane, M. F. Anjos, and S. Le Digabel, "Tight-and-cheap conic relaxation for the ac optimal power flow problem," *IEEE Trans. Power Syst.*, vol. 33, no. 6, pp. 7181–7188, Nov. 2018.
[29] E. Dall'Anese, H. Zhu, and G. B. Giannakis, "Distributed optimal power flow for smart microgrids," *IEEE Trans. Smart Grid*, vol. 4, no. 3, pp. 1464–1475, Sep. 2013.
[30] L. Gan and S. H. Low, "Convex relaxation and linear approximation for optimal power flow in multiphase radial networks," in *Proc. Power Syst. Comput. Conf. (PSCC)*, 2014, pp. 1–9.
[31] C. Zhao, E. Dall'Anese, and S. Low, "Convex relaxation of opf in multiphase radial networks with delta connection," in *Proc. 10th Bulk Power Syst. Dyn Control Symp.*, 2017.
[32] Y. Liu, J. Li, L. Wu, and T. Ortmeyer, "Chordal relaxation based ACOPF for unbalanced distribution systems with DERs and voltage regulation devices," *IEEE Trans. Power Syst.*, vol. 33, no. 1, pp. 970–984, Jan. 2018.
[33] W. Wang and N. Yu, "Chordal conversion based convex iteration algorithm for three-phase optimal power flow problems," *IEEE Trans. Power Syst.*, vol. 33, no. 2, pp. 1603–1613, Aug. 2017.
[34] D. K. Molzahn, B. C. Lesieutre, and C. L. DeMarco, "Approximate representation of zip loads in a semidefinite relaxation of the opf problem," *IEEE Trans. Power Syst.*, vol. 29, no. 4, pp. 1864–1865, Jan. 2014.
[35] R. Benato, A. Paolucci, and R. Turri, "Power flow solution by a complex admittance matrix method," *Eur. Trans. Electr. Power*, vol. 11, no. 3, pp. 181–188, 2001.
[36] K. Sunderland, M. Coppo, M. Conlon, and R. Turri, "A correction current injection method for power flow analysis of unbalanced multiple-grounded 4-wire distribution networks," *Electr. Power Syst. Res.*, vol. 132, pp. 30–38, Mar. 2016.
[37] W. H. Kersting, *Distribution System Modeling and Analysis*, 2nd ed. Boca Raton, FL, USA: CRC Press, 2007.
[38] J. Csatár and A. Dán, "Novel load flow method for networks with multipoint-grounded-neutral and phase-to-neutral connected equipment," *Int. J. Electr. Power Energy Syst.*, vol. 107, pp. 726–734, May 2019.
[39] F. Bignucolo, R. Caldon, M. Coppo, and R. Turri, "Effects of distributed generation on power losses in unbalanced low voltage networks," in *Proc. IEEE Power Energy Soc. General Meeting*, Aug. 2018, pp. 1–5.
[40] W. H. Kersting, "Radial distribution test feeders," in *Proc. IEEE Power Eng. Soc. Winter Meeting*, vol. 2, Aug. 2001, pp. 908–912.
[41] Study Committee C6, "Benchmark systems for network integration of renewable and distributed energy resources," CIGRE, Tech. Rep. T. F. C6.04.02.
[42] M. Usman, M. Coppo, F. Bignucolo, R. Turri, and A. Cerretti, "A novel methodology for the management of distribution network based on neutral losses allocation factors," *Int. J. Electr. Power Energy Syst.*, vol. 110, pp. 613–622, Sep. 2019.
[43] J. Löfberg, "Yalmip: A toolbox for modeling and optimization in MATLAB," in *Proc. CACSD Conf.*, Taipei, Taiwan, 2004, pp. 284–289.
[44] S. Bose, S. H. Low, T. Teeraratkul, and B. Hassibi, "Equivalent relaxations of optimal power flow," *IEEE Trans. Autom. Control*, vol. 60, no. 3, pp. 729–742, Mar. 2015.
[45] A. Venzke, S. Chatzivasileiadis, and D. K. Molzahn, "Inexact convex relaxations for AC optimal power flow: Towards AC feasibility," 2019, *arXiv:1902.04815*. [Online]. Available: https://arxiv.org/abs/1902.04815
[46] K. Yamashita, S. Djokic, J. Matevosyan, F. Resende, L. Korunovic, Z. Dong, and J. Milanovic, "Modelling and aggregation of loads in flexible power networks–scope and status of the work of cigre wg c4. 605," *IFAC Proc. Volumes*, vol. 45, no. 21, pp. 405–410, 2012.
[47] C. Coffrin, H. L. Hijazi, and P. Van Hentenryck, "Strengthening the SDP relaxation of AC power flows with convex envelopes, bound tightening, and valid inequalities," *IEEE Trans. Power Syst.*, vol. 32, no. 5, pp. 3549–3558, Sep. 2017.
[48] A. Wächter and L. T. Biegler, "On the implementation of an interior-point filter line-search algorithm for large-scale nonlinear programming," *Math. Program.*, vol. 106, no. 1, pp. 25–57, 2006.
[49] J. Currie and D. I. Wilson, "OPTI: Lowering the barrier between open source optimizers and the industrial MATLAB user," in *Foundations of Computer-Aided Process Operations*, N. Sahinidis and J. Pinto, Eds. Savannah, GA, USA, Jan. 2012.
[50] P. E. Gill, W. Murray, and M. A. Saunders, "SNOPT: An SQP algorithm for large-scale constrained optimization," *SIAM Rev.*, vol. 47, no. 1, pp. 99–131, 2005.
[51] J. F. Sturm, "Using SeDuMi 1.02, a MATLAB toolbox for optimization over symmetric cones," *Optim. Methods Softw.*, vol. 11, nos. 1–4, pp. 625–653, 1999.
[52] R. H. Tütüncü, K.-C. Toh, and M. J. Todd, "Solving semidefinite-quadratic-linear programs using sdpt3," *Math. Program.*, vol. 95, no. 2, pp. 189–217, 2003.
[53] J. Mareček and M. Takáňc, "A low-rank coordinate-descent algorithm for semidefinite programming relaxations of optimal power flow," *Optim. Methods Softw.*, vol. 32, no. 4, pp. 849–871, 2017.

[54] J. Liu, A. C. Liddell, J. Marecek, and M. Takáˇvc, "Hybrid methods in solving alternating-current optimal power flows," *IEEE Trans. Smart Grid*, vol. 8, no. 6, pp. 2988–2998, Jun. 2017.
[55] R. Madani, A. Kalbat, and J. Lavaei, "ADMM for sparse semidefinite programming with applications to optimal power flow problem," in *Proc. 54th IEEE Conf. Decis. Control (CDC)*, Dec. 2015, pp. 5932–5939.
[56] Q. Peng and S. H. Low, "Distributed optimal power flow algorithm for radial networks, I: Balanced single phase case," *IEEE Trans. Smart Grid*, vol. 9, no. 1, pp. 111–121, Apr. 2018.
[57] R. Louca, P. Seiler, and E. Bitar, "A rank minimization algorithm to enhance semidefinite relaxations of optimal power flow," in *Proc. IEEE 51st Annu. Allerton Conf. Commun., Control, Comput. (Allerton)*, Oct. 2013, pp. 1010–1020.
[58] R. Madani, S. Sojoudi, G. Fazelnia, and J. Lavaei, "Finding low-rank solutions of sparse linear matrix inequalities using convex optimization," *SIAM J. Optim.*, vol. 27, no. 2, pp. 725–758, 2017.

MUHAMMAD USMAN (M'19) received the B.Sc. degree (Hons.) in electrical engineering from UET, Lahore, Pakistan, in 2011, and the M.Sc. degree in power engineering, with main focus on the application of power electronics in electrical drives, from the Technical University of Munich, Germany, in 2016. He is currently pursuing the Ph.D. degree in electric energy engineering with the University of Padova, Italy. His main research interests include modeling, control, and optimization of power systems, as well as the analysis of the role of distributed energy resources in the management of medium and low voltage distribution networks.

ANDREA CERVI (M'19) was born in Montebelluna, Italy. He received the B.Sc. and M.Sc. degrees in electrical energy engineering from the University of Padova, Italy, in 2015 and 2018, respectively. He is currently working as a Research Fellow with the Interdepartmental Centre Giorgio Levi Cases for Energy Economics and Technology. His main research works are distribution network stability, microgrid protections, and renewable energy source integration.

MASSIMILANO COPPO (M'16) received the Ph.D. degree in electrical energy engineering from the University of Padova, Italy, in 2016. He is currently a Research Associate with the University of Padova. His main research interests include modeling and simulation of power systems for smart grid management and energy markets participation, network stability, and power quality analysis related to integration of distributed resources in electrical networks.

FABIO BIGNUCOLO is currently a Research Fellow with the Department of Industrial Engineering, University of Padova. He is also working on network applications for electrochemical storage units aiming at providing ancillary services to the transmission and distribution grids. He is the author or coauthor of more than 50 articles presented at national and international conferences or published on esteemed international journals. His research interests especially concern computer applications in electrical power engineering, regulation of distribution networks hosting dispersed generators, innovative control architectures, and modeling of components and plants.

ROBERTO TURRI was born in Padova, Italy, in 1958. He received the Dr.Ing. degree in electrical engineering from the University of Padova, Italy, in 1984, and the Ph.D. degree from the University of Wales, in 1987. He was with the Physics Department, University College of Swansea, Wales, U.K. In 1990, he joined the Electrical Engineering Department, University of Padova, where he is currently working as an Associate Professor in power systems. His main research interests include the fields of power system analysis and simulation, smart grids, and assessment and mitigation of human exposure to low frequency electromagnetic fields.